Neotectonics of the Sumatran fault, Indonesia

Sieh, Kerry; Natawidjaja, Danny H.

2000

Sieh, K., & Natawidjaja, D. (2000). Neotectonics of the Sumatran fault, Indonesia. Journal of Geophysical Research, 105, 28295–28326.

https://hdl.handle.net/10356/95544

https://doi.org/10.1029/2000JB900120

JOURNAL OF GEOPHYSICAL RESEARCH, VOL. 105, NO. B12, PAGES 28,295–28,326, DECEMBER 10, 2000

Neotectonics of the Sumatran fault, Indonesia

Kerry Sieh

Seismological Laboratory, California Institute of Technology, Pasadena

Danny Natawidjaja[1]

Geoteknologi, Lembaga Ilmu Pengetahuan Indonesia, Bandung, Indonesia

Abstract. The 1900-km-long, trench-parallel Sumatran fault accommodates a significant amount of the right-lateral component of oblique convergence between the Eurasian and Indian/Australian plates from 10°N to 7°S. Our detailed map of the fault, compiled from topographic maps and stereographic aerial photographs, shows that unlike many other great strike-slip faults, the Sumatran fault is highly segmented. Cross-strike width of step overs between the 19 major subaerial segments is commonly many kilometers. The influence of these step overs on historical seismic source dimensions suggests that the dimensions of future events will also be influenced by fault geometry. Geomorphic offsets along the fault range as high as ~20 km and may represent the total offset across the fault. If this is so, other structures must have accommodated much of the dextral component of oblique convergence during the past few million years. Our analysis of stretching of the forearc region, near the southern tip of Sumatra, constrains the combined dextral slip on the Sumatran and Mentawai faults to be no more than 100 km in the past few million years. The shape and location of the Sumatran fault and the active volcanic arc are highly correlated with the shape and character of the underlying subducting oceanic lithosphere. Nonetheless, active volcanic centers of the Sumatran volcanic arc have not influenced noticeably the geometry of the active Sumatran fault. On the basis of its geologic history and pattern of deformation, we divide the Sumatran plate margin into northern, central and southern domains. We support previous proposals that the geometry and character of the subducting Investigator fracture zone are affecting the shape and evolution of the Sumatran fault system within the central domain. The southern domain is the most regular. The Sumatran fault there comprises six right-stepping segments. This pattern indicates that the overall trend of the fault deviates 4° clockwise from the slip vector between the two blocks it separates. The regularity of this section and its association with the portion of the subduction zone that generated the giant (M_W 9) earthquake of 1833 suggest that a geometrically simple subducting slab results in both simple strike-slip faulting and unusually large subduction earthquakes.

1. Introduction

1.1. Plate Tectonic Environment

The Sumatran fault belongs to a class of trench-parallel strike-slip fault systems that work in concert with subduction zones to accommodate obliquely convergent plate motion [*Yeats et al.*, 1997, Chapter 8]. Other strike-slip faults that occur in similar settings include the left-lateral Philippine fault (parallel to the Luzon and Philippine trenches), Japan's right-lateral Median Tectonic Line (parallel to the Nankai trough), and Chile's Atacama fault (parallel to the South American trench).

For its entire 1900-km length the Sumatran fault traverses the hanging wall block of the Sumatran subduction zone, roughly coincident with the active Sumatran volcanic arc (Figure 1). On its northeastern side is the southeast Asian plate, separated from the Eurasian plate only by the slow slipping Red River fault of Vietnam and southern China [*Allen et al.*, 1984]. On its southwestern side is the Sumatran "forearc sliver plate" [*Jarrard*, 1986], a 300-km-wide strip of lithosphere between the Sumatran fault and the Sumatran deformation front. At its northwestern terminus the Sumatran fault transforms into the spreading centers of the Andaman Sea [*Curray et al.*, 1979]. At its southeastern end, in the Sunda Strait, the fault curves southward toward the deformation front [*Diament et al.*, 1992].

The basic kinematic role of the Sumatran fault is rather simple: It accommodates a significant amount of the strike-slip component of the oblique convergence between the Australian/Indian and Eurasian plates. The pole of rotation for the relative motion between the Australian/Indian and Eurasian plates is in east Africa, ~50° west of Sumatra [*Prawirodirdjo et al.*, this issue, *Prawirodirdjo*, 2000; *Larson et al.*, 1997]. Northern Sumatra is closer to this pole than is southern Sumatra. Thus the orientation and magnitude of the relative-motion vector vary significantly along the Sumatran

[1]Now at Division of Geological and Planetary Sciences, California Institute of Technology, Pasadena.

Paper number 2000JB900120.
0148-0227/00/2000JB900120$09.00

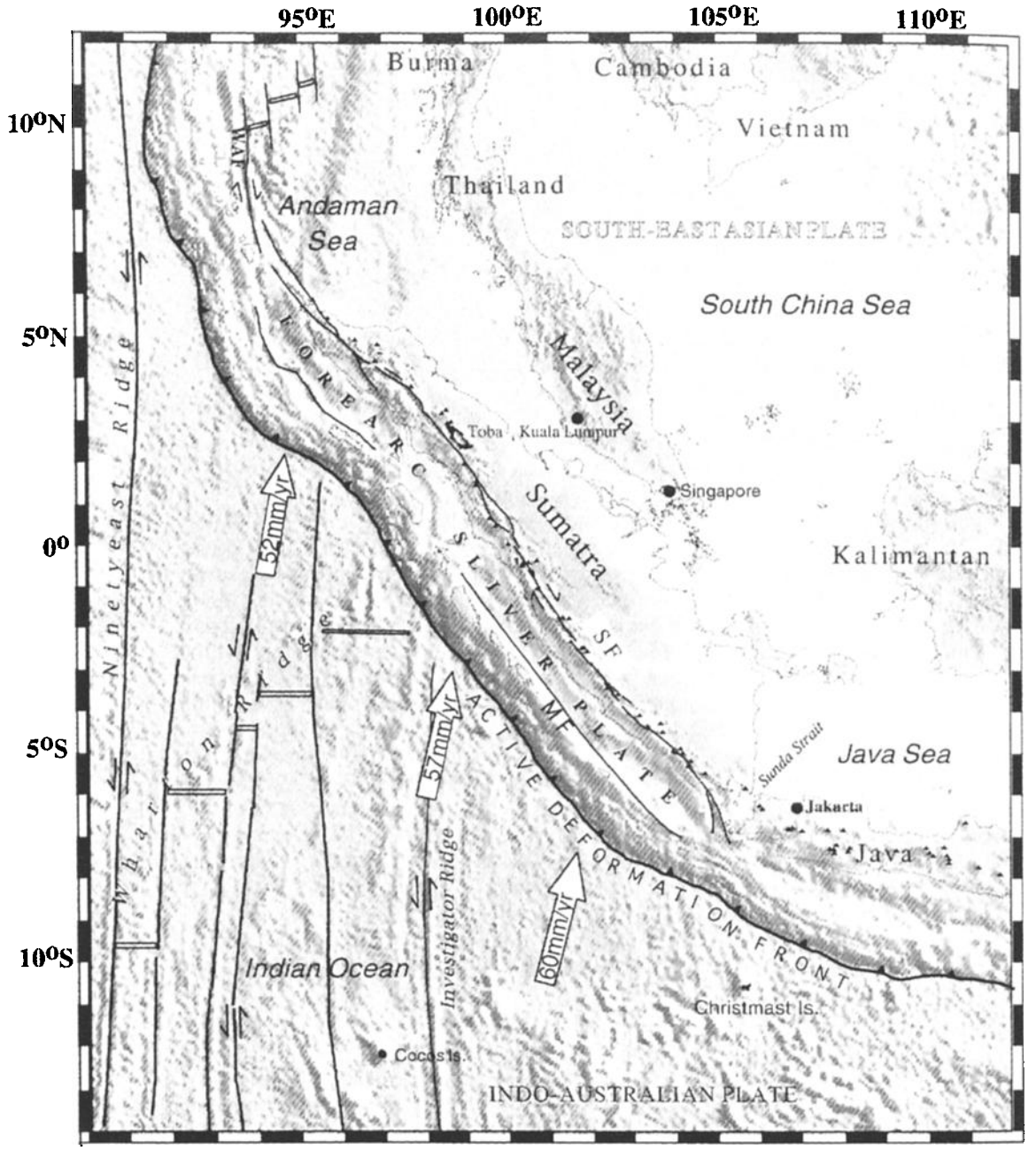

Figure 1. Regional tectonic setting of the Sumatran fault . The Sumatran fault (SF) is a trench-parallel, right-lateral strike-slip fault that traverses the hanging wall block of the Sumatran subduction zone from the Sunda Strait to the spreading centers of the Andaman Sea. It separates a forearc sliver plate from the southeast Asian plate. Triangles are active volcanoes of the Sunda arc. Arrow is relative plate motion vectors determined from GPS. Topography and bathymetry are from *Smith and Sandwell* [1997]. WAF is the West Andaman fault. MF is the Mentawai fault.

portion of the plate boundary (Figure 1). At 6°S, 102°E it is 60 mm/yr, N17°E [*Prawirodirdjo et al.*, this issue]. At 2°N, 95°E, it is 52 mm/yr, N10°E. Furthermore, because the shape of the plate boundary is arcuate, the nature of relative plate motion changes markedly along its strike. At the longitude of central Java the strike of the subduction zone is nearly orthogonal to the direction of relative plate motion, so any component of strike-slip motion need not be large [*McCaffrey*, 1991]. At the latitudes of Sumatra, however, the strike-slip component of relative plate motion must be significant because the direction of relative plate motion is substantially oblique to the strike of the subduction zone.

Fitch [1972] suggested that the right-lateral component of this oblique convergence is the cause for the right-lateral Sumatran fault. *McCaffrey* [1991, 1992] added more substance to this hypothesis with his discovery that slip vectors of moderate earthquakes along the Sumatran portion of the subduction zone are nearly perpendicular to the strike of the plate boundary. He noted that if these vector directions are representative of long-term slip trajectories along the subduction interface, then subduction itself is only slightly oblique and most of the dextral component of plate motion must be accommodated elsewhere.

The Sumatran fault is the most obvious candidate for

accommodation of the remaining component of dextral slip. The Mentawai fault, discovered offshore by *Diament et al.* [1992], complicates this slightly. This major, submarine, trench-parallel fault lies between the Sumatran fault and the trench and may also have accommodated a significant amount of the dextral component of plate motion.

The combination of an arcuate plate boundary and a distant pole of rotation suggests that the rate of dextral slip along the Sumatran fault increases northwestward [*Huchon and Le Pichon,* 1984; *McCaffrey,* 1991]. Observations near the northwestern and southeastern termini of the Sumatran fault support this contention. *Curray et al.* [1979] suggested that the rate of opening across the spreading centers of the Andaman Sea (Figure 1) has averaged about 37 mm/yr for the past 11 Myr. They proposed that most of this motion has been carried to the southeast by the Sumatran fault. Reanalysis of these data yields the same rate; total opening in the past 3.2 Myr is ~118 km (J. Curray, written communication, 1999). The slip rate inferred for the Sumatran fault near its southern terminus, however, appears to be far lower than 37 mm/yr. *Bellier et al.* [1999] calculate a rate of ~6 mm/yr near the southern end of the fault from an offset channel incised into a dated Pleistocene tuff.

1.2. Motivation of This Work

Despite its ranking as one of Earth's great strike-slip faults, its high level of historical seismic activity and its major role in the active tectonics and seismic hazard of Southeast Asia, the Sumatran fault has not been well characterized. What attention the fault has received has been predominantly from a great distance, mostly at plate tectonic scales. Until recently, the geometry of the fault was known only to first-order (see, for example, the small-scale maps of *Fitch* [1972], *Bellier et al.* [1997] or *McCaffrey* [1991]. More detailed studies have been limited to local studies, such as *Tija's* [1977] and *Katili and Hehuwat's* [1967] work on exemplary offset drainages.

The Sumatran fault has generated many historical earthquakes with magnitudes M≥ 7, but because most of these happened more than a half a century ago, they have not been well documented. *Reid* [1913] used geodetic measurements from before and after the 1892 Sumatran earthquake as support for his concept of elastic rebound. *Berlage* [1934] described the effects of the 1933 earthquake in south Sumatra. *Visser* [1927] described the effects of the 1926 Padangpanjang earthquake in west Sumatra, and *Untung et al.* [1985] and *Natawidjaja et al.* [1995] recently reported dextral offsets formed during the nearby 1943 Alahanpanjang earthquake.

The paucity of detailed maps of the fault, the scarcity of data on historical large earthquakes, and the lack of reliable estimates of slip rates are unfortunate. They seriously hamper attempts to forecast the seismic productivity of the fault and efforts to understand quantitatively its role in the oblique convergence of the Sumatran plate boundary.

Our first task in this study, then, has been to construct a modern map of the active components of the Sumatran fault. To be of use in seismic hazard assessment and in understanding the neotectonic role of the fault, the scale of the map needed to be large enough to clearly discriminate major fault strands and the discontinuities and changes in strike between strands.

Our second task, which will be described in a future paper, will be to determine the slip rate of the fault at several localities to determine whether or not the actual slip rates conform to current kinematic models. Such rates would also serve as a long-term average for the interpretation of geodetic data from Global Positioning System (GPS) networks that now span the fault [*Genrich et al.*, this issue] and historical triangulation data [*Prawirodirdjo et al.*, this issue].

2. A Modern Map of the Fault

To map the Sumatran fault efficiently and reliably, we have relied primarily upon its geomorphic expression. Geomorphic expression is especially reliable for mapping high slip rate faults, where tectonic landforms commonly develop and are maintained at rates that exceed local rates of erosion or burial [*Yeats et al.*, 1997, Chapter 8]. Examples of geomorphologically based regional maps of active faults include active fault maps of Japan, Turkey, China, Tibet, and Mongolia [*Research Group for Active Faults*, 1980; *Saroglu et al.*, 1992; *Tapponnier and Molnar*, 1977] as well as most maps of submarine active faults.

Admittedly, the geomorphic expression of active faults with slip rates that are lower than or nearly equal to local rates of erosion or burial is likely to be obscure. This is especially likely if the faults are short, have small cumulative offset, or have no component of vertical motion. Because of our reliance on geomorphic expression, our map of the Sumatran fault undoubtedly excludes many short, low-rate active fault strands.

2.1. Resources and Methods

The grossest features of the Sumatran fault have long been known from analysis of small-scale topographic and geologic maps. More detailed small-scale maps of the fault, based upon analysis of satellite imagery, have been produced more recently [*Bellier et al.*, 1997; *Bellier and Sebrier*, 1994; *Detourbet et al.*, 1993]. The unavailability of stereographic imagery, however, limited the resolution and the reliability of these small-scale maps. Specifically, the lack of stereoscopic coverage precluded the recognition of important small tectonic landforms, unless they were favorably illuminated. Conversely, inactive faults lacking small, late Pleistocene and Holocene tectonic landforms may have been mapped as active, based upon the presence of older and larger tectonic landforms.

Our mapping of the Sumatran fault is based primarily upon inspection of 1:50,000-scale topographic maps and 1:100,000-scale aerial photographs. Where these were not available or were of unsuitable quality, we utilized 1:250,000-scale geologic maps and radar imagery. Figure 2 displays the coverage of materials that we used.

Figure 3 displays representative stereographic pairs of the 1:100,000-scale aerial photographs. These photos display the fault at about 0.3°S, where it offsets stream channels that are deeply incised into a thick pyroclastic flow deposit. After interpreting these and other stereopairs, we compiled our interpretations onto 1:50,000-scale topographic maps (or 1:250,000-scale topographic maps, where the larger-scale maps were unavailable). Where stereographic aerial photographs were unavailable, we interpreted active fault geometry and sense of slip directly from the 1:50,000-scale topographic maps.

These data were then digitized and attributed, using the Geographic Information System (GIS) software, Arc/Info.

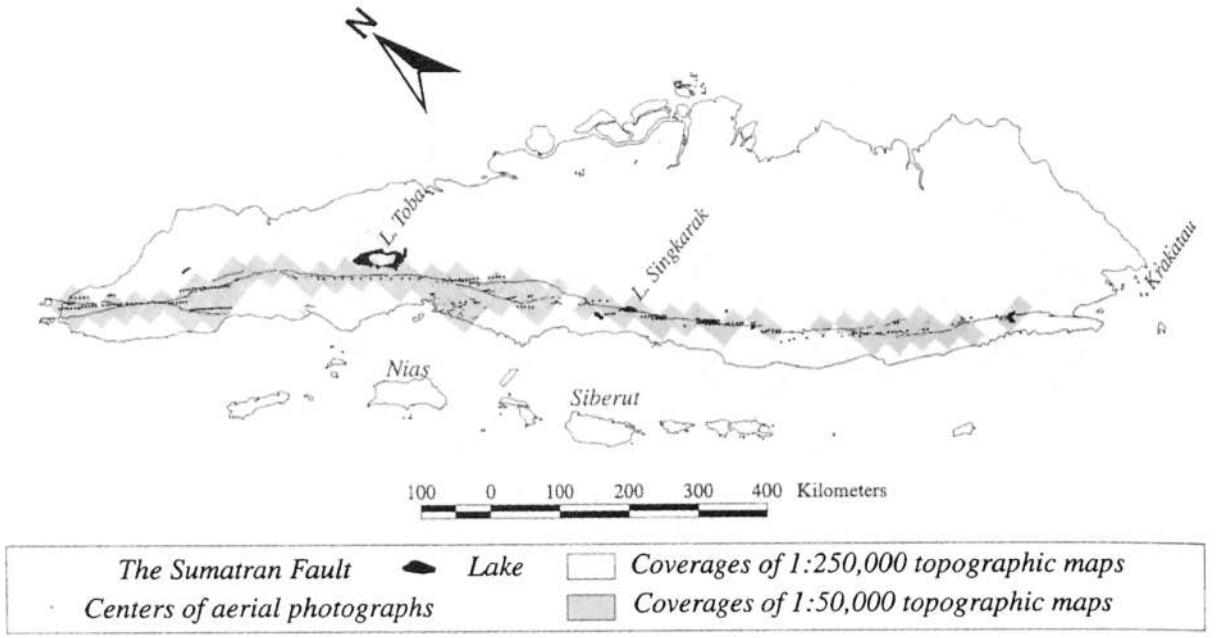

Figure 2. Data upon which our map compilation is based. Most of our mapping is based on inspection of 1:50,000-scale topographic maps produced by BAKOSURTANAL & JANTOP, the national mapping agencies for Indonesia, and 1:100,000-scale aerial photographs. Other data sources include smaller-scale geologic and topographic maps.

The resulting GIS database includes fault geometry, sense of fault slip, and photo centers. Plate 1, constructed from the database, depicts all of the salient features of the Sumatran plate boundary that we mapped and compiled.

2.2. Geometry of the Fault

The overall shape of the Sumatran fault across Sumatra is sinusoidal (Figure 1). The northern half of the fault is gently concave to the southwest, whereas the southern half of the fault is concave to the northeast. Over the 1650-km subaerially exposed length of the fault, the "amplitude" of the sinusoidal trace is ~55 km.

Ornamenting the broad, sinusoidal shape of the Sumatran fault are numerous smaller irregularities. Though smaller, these have dimensions of the order of tens of kilometers and are therefore tectonically and seismologically significant.

The greatest of these is a feature that we call the Equatorial Bifurcation (Figure 1 and Plate 1). This forceps-shaped feature is present between the equator and about 1.8°N latitude. It is characterized by the bifurcation of the Sumatran fault toward the southeast into two principal active strands. The two strands are distinct from each other even at their point of bifurcation (about 1.8°N). The greatest separation of these two branches is ~35 km, near 0.7°N. The western branch of the bifurcation does not rejoin the eastern branch farther south; instead, it dies out geomorphically at about 0.35°N.

Other large irregularities include subparallel geomorphically expressed fault traces at about 5.5°N, 4°N, and 3.5°S. The Batee fault, a right-lateral fault that may have displaced the island's western shelf ~150 km since the Oligocene [*Karig et al.*, 1980], diverges southward from the Sumatran fault at about 4.6°N. A 75-km-long fold-and-thrust belt, exhibiting clear geomorphic evidence of youthfulness lies about 40 km west of the Sumatran fault at about 1.3°N. All of these features are described in section 2.3.

2.3. Major Segments of the Sumatran Fault

Superimposed upon the broad sinusoidal geometry of the Sumatran fault are more than a dozen discontinuities, ranging in width from ~5 to 12 km (Plate 1). Major local changes in strike also occur. Most of the discontinuities are right steps in the fault trace and thus represent dilatational step overs. However, a few contractional bends also occur. Theoretically, these discontinuities and bends in the fault are large enough to influence the seismic behavior of the fault [*Harris et al.*, 1991; *Harris and Day*, 1993]. The relationship of historical ruptures to these geometrical segment boundaries will be the subject of a future paper (D. Natawidjaja and K. Sieh, manuscript in preparation,2000).

We have used these second-order geometric irregularities to divide the Sumatran fault into 19 segments (Figure 4 and Table 1). Each segment bears the name of a major river or bay along the segment. In so naming the various segments, we have abandoned the usual practice of retaining names that have precedence in the scientific literature. The nomenclatural morass inherited from numerous earlier studies includes many fault names derived from nearby cities, districts, basins, and rivers. These include Banda Aceh Anu, Lam Teuba Baro, Reuengeuet Blangkejeren, Kla-Alas, Ulu-Aer, Batang-Gadis, Kepahiang-Makakau, Ketahun, Muara Labuh, and Semangko [e.g., see *Katili and Hehuwat*, 1967; *Cameron et al.*, 1983; *Durham*, 1940]. Since many of these overlap our geometric segment boundaries or include only parts of our segments, we have abandoned them in favor of a more systematic and precise nomenclature.

For the entire group of active fault segments, from Aceh in the north to the Sunda Strait in the south, we have chosen the name "Sumatran fault," first used by *Katili and Hehuwat* [1967]. This name represents best the dimension of the structure. Earlier names for the fault are "Semangko" and "Ulu-Aer," suggested by *Van Bemmelen* [1949] and *Durham* [1940]; but these refer to local features. "Great Sumatran

THE SUMATRAN FAULT SYSTEM, INDONESIA

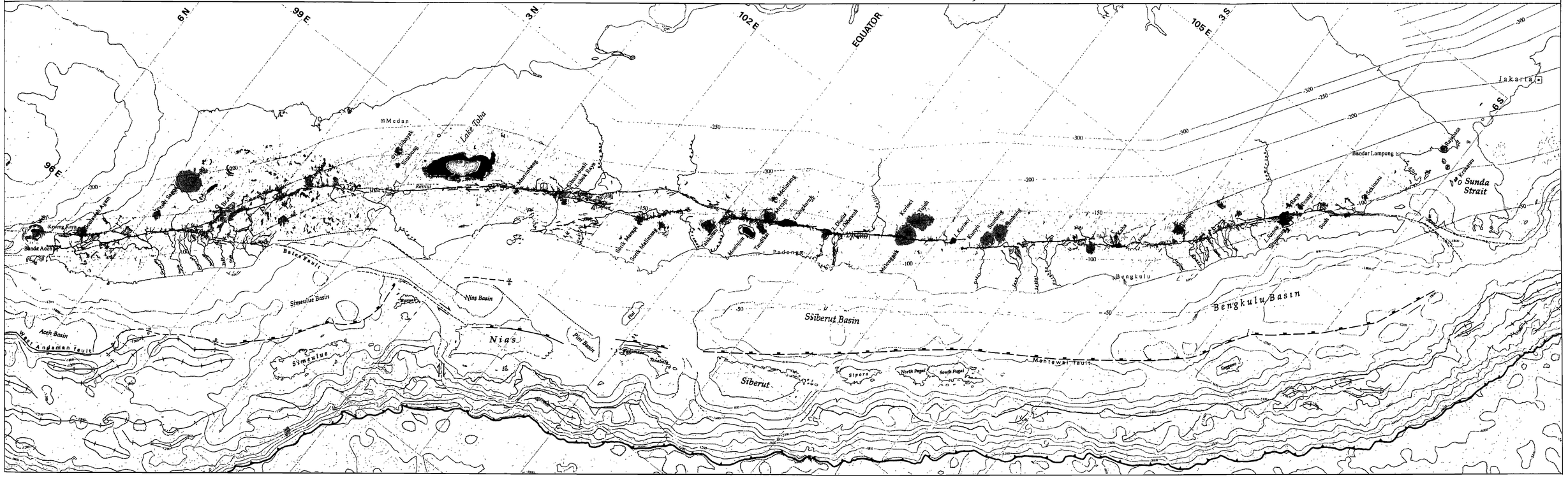

Active Faults, dashed where approximated, dotted where concealed
Active strike-slip faults
Active faults with reverse component
Active faults with normal component
Anticline; dashed where approximated
Syncline; dashed where approximated

Faults with no indication of recent activity, dashed where approximated
strike-slip faults
Faults with normal component
Faults with dip-slip components; U=up, D=down
Homocline

Faults of inner trench slope, current activity unknown
Folds of inner trench slope, current activity unknown
Active deformation front
-100 Isobath of the Benioff-Wadati Zone
Axes of forearc basins
Axes of outerarc ridges

Volcano: crater & cone
Caldera
Valleys / depressions
Lake
Contours of elevation; created from 30 second grid DEM - GTOPO30
Interval contours : 100 & 500 meters
Contours of bathymetry; created from 2 minute grid DEM
Etopo2 (Smith & Sandwell, 1997); Interval contour : 200 & 600 meters

Date : September 11, 2000

0 50 100 150 200
Kilometers

Kerry Sieh & Danny Natawidjaja
Division of Geological and Planetary Sciences, Caltech

Plate 1. Map of the Sumatran fault and related features. (This map and its GIS database are available at www.sceodc.scec/geologic/sumatra.)

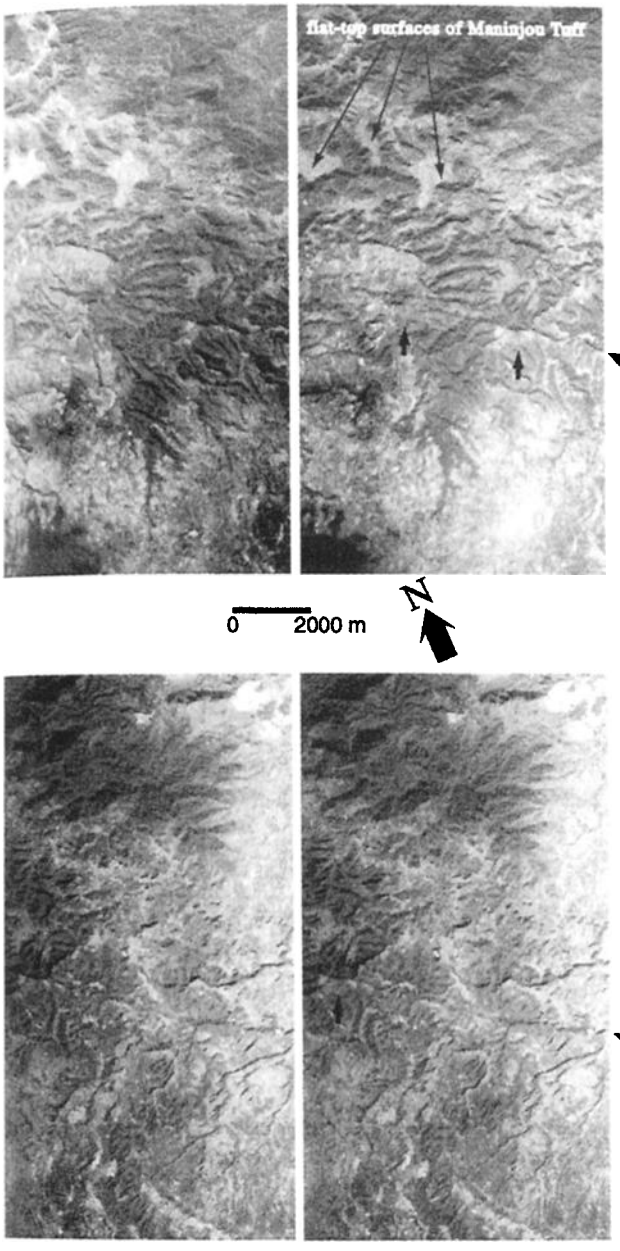

Figure 3. An example of the approximately 1:100,000-scale aerial photographs we used to compile most of our map of the Sumatran fault. These two sets of stereopairs show channel offsets of ~720 m. The channels cut a late Pleistocene pyroclastic flow deposit at about 0.3°S. The flat upland surfaces are the unincised top of the flow. These offsets yield a average slip rate of ~11 mm/yr.

trough system" was first used by *Westerveld* [1953]. Since "great" is not used for other faults of similar dimension, we suggest that it not be used for the Sumatran fault. In keeping with convention generally accepted in California, where "San Andreas fault system" refers to the San Andreas and its many auxiliary faults, we use "Sumatran fault system" (SFS) for the Sumatran fault and other structures that are related to the accommodation of strike slip along the Sumatran plate margin. These would include the Batee fault, the Toru fold-and-thrust belt, and the Mentawai and the West Andaman faults in the forearc region (Figure 1). For discrete, individual segments along the Sumatran fault, we suggest the particular names in Figure 4.

In sections 2.3.1-2.3.19, we describe each segment, beginning in the south. Each description focuses on the geomorphic expression of the segment and its terminations. Discussion of important historical earthquakes is minimal because the association of earthquakes with segments will be the focus of a future paper. Likewise, we do not focus on the slip rates of the various segments because this also will be the principal topic of a future paper.

Plate 1 displays the fault at a scale that is appropriate for the detailed discussion that follows. (This plate and it's database are also available as postscript and GIS (ArcView) files at www.scecdc.scec.org/geologic/sumatra).

2.3.1. Sunda segment (6.75°S to 5.9°S). Bathymetric maps of the Sunda Strait, between Java and Sumatra, reveal that the southernmost portion of the Sumatran fault is associated with two prominent south striking fault scarps on the seafloor [*Nishimura et al.*, 1986; *Zen et al.*, 1991; *Pramumijoyo and Sebrier*, 1991]. These scarps form a submarine graben, ranging in depth to 1800 below sea level (Figure 5). The large vertical displacements of the seafloor and the orientation and location of the faults suggest that their sense of slip is normal and dextral. Focal mechanisms from a local seismic network [*Harjono et al.*, 1991] and from the Harvard Centroid Moment Tensor (CMT) catalogue support this interpretation. They show normal-fault mechanisms on the western side of the graben. Furthermore, faults appear on both sides of the graben in three seismic reflection profiles [*Lassal et al.*, 1989].

The graben widens southward, toward the subduction zone, but loses bathymetric expression ~130 km from the trench, near where one would expect it to intersect the floor of the Sumatran and Javan forearc basins (Figure 5). A belt of fault scarps and folds of the inner trench slope continues across the southward projection of the graben, but the outer-arc ridge and forearc basin that are prominent in the offshore of Sumatra and Java are absent in this region. Instead, these features appear to converge upon each other and to be replaced by a narrow, 150-km-long plateau across the projection of the graben. The lessening of sliver-plate width occasioned by the absence of the forearc basin and outer-arc ridge appears to be accommodated by a landward deflection of the trench axis (Figures 1 and 5).

Huchon and Le Pichon [1984] were the first to propose that the disappearance of the outer-arc ridge and the forearc basin across the southern projection of the Sumatran fault indicates stretching parallel to the Sumatran fault. They also speculated that the subtle bending of the trench toward the Sunda Strait indicates arc-normal thinning of the region between the trailing edge of the Sumatran forearc sliver plate and the crust offshore from Java. This would be consistent with the northwestward translation of the forearc sliver plate along the Sumatran fault. We attempt to quantify this stretching in section 3.

2.3.2. Semangko segment (5.9°S to 5.25°S). From beneath the waters of Semangko Bay at about 5.9°S to a 6-km-wide dilatational step over that has produced the Suoh Valley at about 5.25°S, the principal trace of the Sumatran fault runs almost linearly along the southwestern side of Semangko Bay and the Semangko Valley (Plate 1 and Figure 4). The prominent northeast facing escarpment along the 65-km length of this segment attests to a significant component of dip slip, southwest side up. An earthquake on July 26,

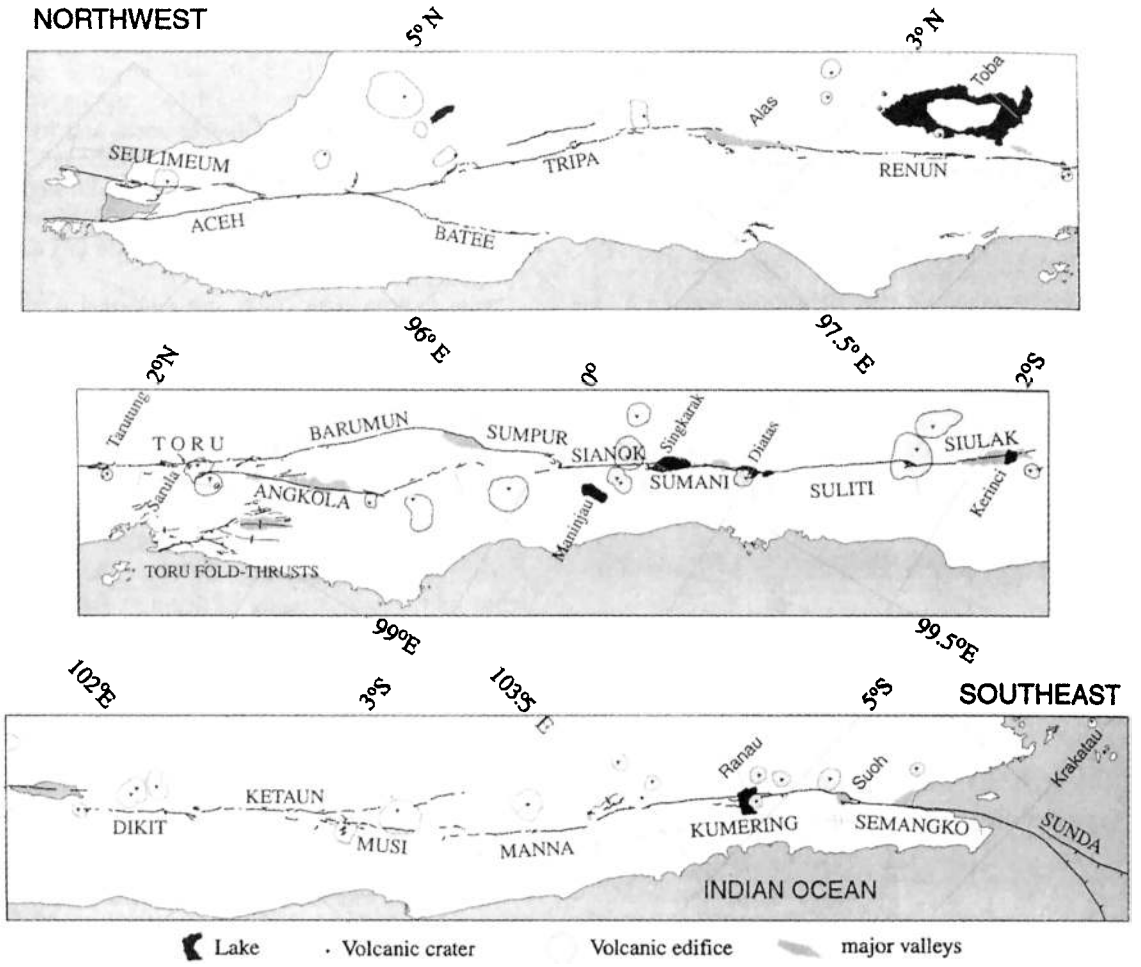

Figure 4. Map of 20 geometrically defined segments of the Sumatran fault system and their spatial relationships to active volcanoes, major graben, and lakes.

1908, may have involved rupture of all or most of this segment [*Berlage*, 1934].

2.3.3. Kumering segment (5.3°S to 4.35°S). This 150-km-long segment runs between the dilatational step over at Suoh Valley to a contractional jog at 4.35°S. Near the center of this segment, the waters of Lake Ranau occupy a late Pleistocene caldera and conceal about 9 km of the trace (Plate 1 and Figure 4). The southern part of the Kumering segment traverses the drainages of the Werkuk and upper Semangko rivers. A less active southeastward continuation of this segment may form the northeastern flank of the Semangko Valley [*Pramumijoyo and Sebrier*, 1991], but we did not have adequate materials to determine its activity there.

North of Lake Ranau, a 40-km-long reach of the fault traverses the headwaters of the Kumering River. The trunk stream of this large river does not cross the fault; instead, its two major tributaries flow toward one another across the trace of the fault and flow northeastward away from the fault from their confluence. This relationship of large stream channels to the fault is common along much of the Sumatran fault; not uncommonly, the headwaters of a principal stream are near the fault, and none of the larger channels of the drainage network cross the fault trace. In these cases, dextral offsets of the stream channels are either ambiguous or small.

The northwesternmost 15 km of the Kumering segment deviates westward from the trend of the rest of the segment and is part of a 10-km-wide contractional jog. This portion of the segment displays a significant component of reverse slip, as evidenced by a high escarpment and a mountainous anticline north of the fault trace. Aerial photography available to us did not reveal the continuation of the fault trace northwest of 4.35°S, through the rest of the contractional bend.

High intensities indicate rupture of many tens of kilometers of the Kumering segment during the Ms 7.5 Liwa earthquake of June 24, 1933 [*Berlage*, 1934]. Deadly phreatic explosions occurred 2 weeks after the earthquake within the Suoh Valley [*Stehn*, 1934].

A geomorphically less prominent subparallel strand of the fault exists 2.5 km to the southwest of the principal active trace south of Lake Ranau [*Natawidjaja*, 1994; *Widiwijayanti et al.*, 1996]. The devastating Mw 6.8 Liwa earthquake of 1994 was generated by this less prominent trace. The most severe damage and the aftershock region coincided with a 25-km reach of this secondary trace.

2.3.4. Manna segment (4.35°S to 3.8°S). This 85-km segment deviates only a kilometer or two from being rectilinear but has rather obscure terminations on both ends

Table 1. The Sumatran Fault's Major Segments

No.	Segment	Latitude	Length, km	Large Historical Earthquakes, year(M)	Nature of Southern Termination	Geomorphic Features	Distance From Deformation Front, km	Depth to Benioff Zone, km
1	Sunda	6.75°S – 5.9°S	~150	No record	submarine forearc	submarine graben	115-220	up to ~50
2	Semangko	5.9°S – 5.25°S	65	1908	southern tip of Semangko Peninsula	east facing scarp	220-270	50-100
3	Kumering	5.3°S – 4.35°S	150	1933(M_s=7.5), 1994(M_w=7.0)	dilatational step over, 6 km width	Suoh geothermal valley	300	100-120
4	Manna	4.35°S – 3.8°S	85	1893	contractional bend, 17^0 deflection	mountainous range on east side of the fault, associated with possible folds and thrusts	275	120
5	Musi	3.65°S – 3.25°S	70	1979 (M_s=6.6)	dilatational step over, 5.6 km width	valley /depression	260	115
6	Ketaun	3.35°S– 2.75°S	85	1943 (M_s=7.3), 1952 (M_s=6.8)	dilatational step over, 5–18.5 km width	depression valley and Kaba volcano	271	110-125
7	Dikit	2.75°S– 2.3°S	60	no record	complex fault discontinuity			
8	Siulak	2.25°S– 1.7°S	70	1909 (M_s=7.6), 1995 (M_w=7.0)	dilatational step over, 11 km width	Lake Kerinci and Kunyit volcano	266	120-130
9	Suliti	1.75°S– 1.0°S	95	1943 (M_s=7.4)	4.5-km-wide dilatational step over	small depression, calderas and young volcanic cone	273	130
10	Sumani	1.0°S – 0.5 °S	60	1943 (M_s=7.6), 1926 (M_s~7)	4.5-km-wide dilatational step over	Lake Diatas, calderas, and Talang volcano	293	130
11	Sianok	0.7°S – 0.1°N	90	1822, 1926 (M_s~7)	4.5-km-wide dilatational step over	Lake Singkarak	302	135–145
12	Sumpur	0° – 0.3°N	35	no record	12-km-wide dilatational step over	wide depression associated with normal faults	308	165–175
13	Barumun	0.3°N – 1.2°N	125	no record	23-km-wide releasing bend	long (Sumpur) valley along the fault	294	125-170
14	Angkola	0.3°N – 1.8°N	160	1892 (M_s=7.7)	complex structure	mountainous ranges on both sides of the fault	290	135–155
15	Toru	1.2°N - 2.0°N	95	1984 (M_s=6.4), 1987 (M_s=6.6)	contractional bend	uplifted hill on the east side of the bend	294	125–155
16	Renun	2.0°N – 3.5°N	220	1916, 1921 (m_b=6.8) 1936 (M_s=7.2)	3-km-wide dilatational step over	Tarutung Valley	286	100–125
17	Tripa	3.4°N – 4.4°N	180	1990 (M_s=6?) 1997 (M_w=6?)	9-km-wide dilatational step over	Alas Valley	295	125–150
18	Aceh	4.4°N – 5.4°N	200	no record	3-km-wide contractional step over	mountainous range, associated with active thrusts	323	105–130
19	Seulimeum	5.0°N – 5.9°N	120	1964 (M_s=6.5)	4-km-wide releasing bend and dilatational step over	small depression on dilatational step over		125–140

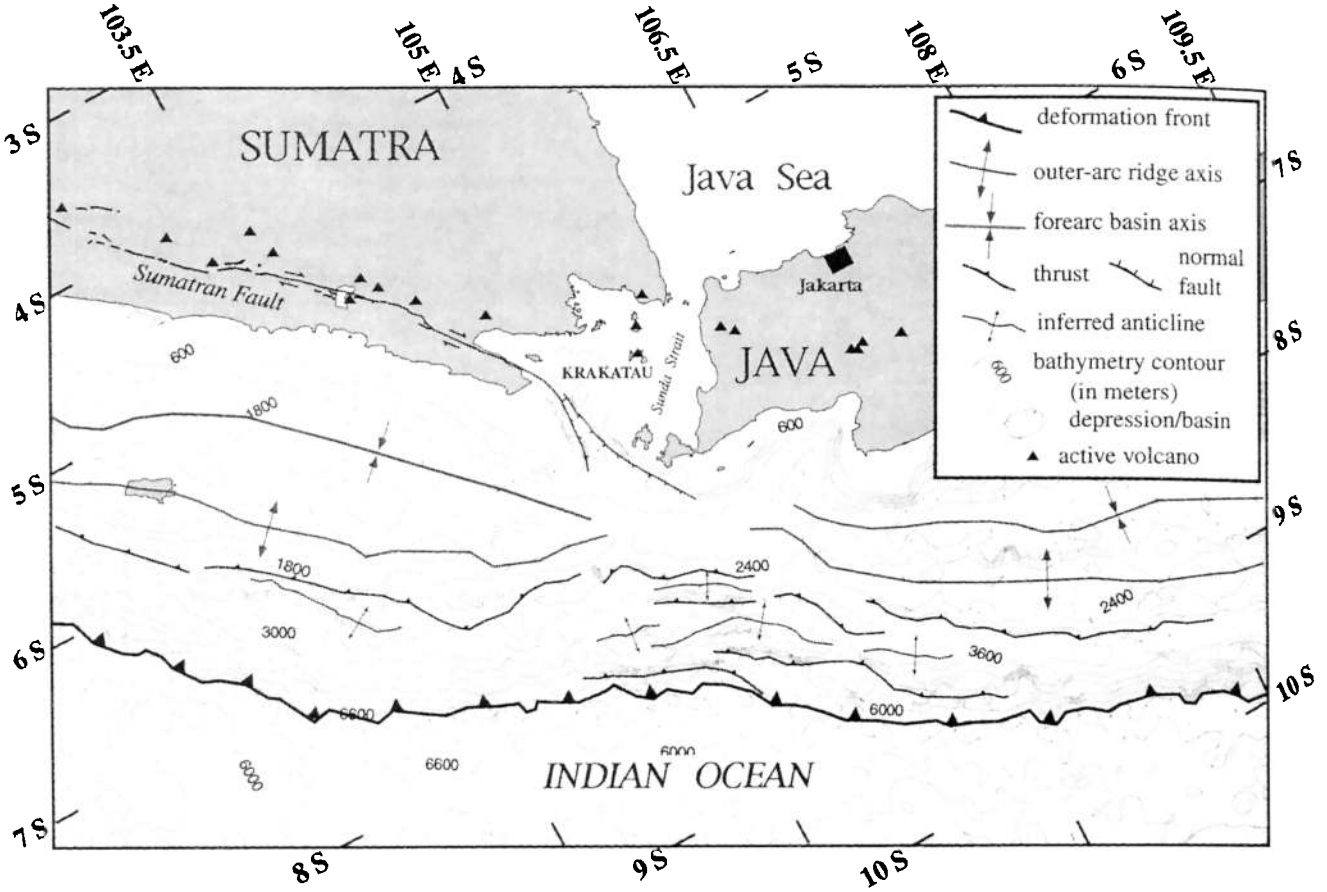

Figure 5. Sumatran fault and related structures near the Sunda Strait and bathymetric map of the portion of the Sunda Strait and surrounding seafloor. The Sunda segment of the Sumatran fault forms an 1800-m-deep graben that widens southward, toward the deformation front. Northwestward movement of the forearc sliver plate along the Sumatran fault appears to have caused thinning of the region between the trench and the strait. Bathymetry is from Digital Elevation Model ETOPO02 and bathymetric surveys [*Smith and Sandwell*, 1997].

(Figure 4). The Manna segment appears discontinuous on Plate 1 because the trace is obscure locally on the aerial photographs and topographic maps. The southern end of the segment abuts the contractional bend mentioned above. The northern end of the segment is obscure beyond about 3.8°S but appears to be within a geometrically complex right (dilatational) step in the fault.

Exceptionally clear 2.4 ± 0.2 km dextral offsets of two large streams (Air Kanan and Air Kiri) exist on the dissected western flank of an extinct volcano southeast of Pajarbulan (Plate 2). We encountered surprisingly well-preserved small tectonic landforms beneath the jungle canopy during an excursion in the drainages of these two streams.

A destructive earthquake occurred in the vicinity of this segment on June 12, 1893. The area of greatest damage coincided with the central part of the Manna segment [*Visser*, 1922].

2.3.5. Musi segment (3.65°S to 3.25°S). This 70-km segment of the Sumatran fault comprises several highly discontinuous fault segments (Figure 4 and Plate 1). Despite good coverage with 1:100,000-scale aerial photography, we could not identify clear geomorphic traces along much of this segment.

The longest continuous trace that we were able to map traverses the southwestern flank of the large, active stratovolcano, Bukit Kaba. Stream channels cut into the youngest flows there are offset ~700 m. We have used these channels to determine the slip rate of 11 mm/yr for the Musi segment (D. Natawidjaja and K. Sieh, manuscript in preparation, 2000).

The destructive, Ms 6.6 Kepahiang earthquake occurred along this segment at about 3.6°S on December 15, 1979. We heard eyewitness accounts of minor cracking along the fault when we visited in 1993, but we saw no convincing evidence of tectonic surficial ruptures from 1979.

2.3.6. Ketaun segment (3.35°S to 2.75°S). This 85-km-long segment consists of a linear trace with several discontinuities and stepovers of about a kilometer in dimension (Plate 1 and Figure 4). The segment's southern end is at a 6- to 8-km-wide dilatational step over onto the Musi segment. An inactive or less active continuation of the Ketaun segment may extend beneath the stratovolcanic edifice of Bukit Kaba. This possibility is suggested by the presence of a geomorphically subdued fault, southeast of the volcano and ~25 km east of the central Musi segment. The northern end of the Ketaun segment is within a 6-km-wide contractional step over. Within this contractional step over the topography rises several hundred meters above the surrounding landscape.

Two major rivers cross the Ketaun segment, the Ketaun in

the south and the Seblat in the north. The Seblat river valley appears to be offset dextrally ~17 km, and the Ketaun river valley may be offset ~23 km. A moderate earthquake on March 15, 1952 (M 6.2, U. S. Geological Survey (USGS)), produced high intensities along the Ketaun segment [*Kraeff*, 1952].

2.3.7. Dikit segment (2.75°S to 2.3°S). This is a predominantly linear, 60-km-long segment with several short, obscure sections along its northern few kilometers (Plate 1 and Figure 4). It shares a contractional step over with the Ketaun segment on its southeastern end. Its northwestern termination is at one of the larger dilatational step overs along the Sumatran fault. On the southwestern flank of this 11-km-wide step over, the Dikit segment disappears into the edifice of the small stratovolcano Kunyit. This is one of the few clear associations of a dilatational step over and a volcano along the Sumatran fault.

The small diamond-shaped caldera of Dipatiampat is offset ~500 m by the fault. Just north of the small caldera lake, at about 2.65°S, the main trace appears to form an enigmatic dogleg. The Dikit River Valley follows the fault for ~20 km. We are not convinced that this represents a dextral offset of 20 km, because the construction of two large volcanic edifices has undoubtedly obscured older drainages on the block northeast of the fault.

2.3.8. Siulak segment (2.25°S to 1.7°S). Clear dilatational step overs demarcate the terminations of this 70-km-long segment (Figure 4 and Plate 1). The 11-km wide stepover at the southeastern end is the widest dilatational step over along the Sumatran fault, but our aerial photography did not reveal its structural details. The northern terminus of the Siulak segment is a 4-km-wide step over on the western flank of the great active stratovolcano Kerinci. West dipping normal faults cut lavas of Melenggok volcano there, and appear to transfer slip from the Siulak segment to its northwestern neighbor.

Along the Siulak segment's southeastern reach, Lake Kerinci and the alluvium of a broad valley obscure the fault trace for ~30 km. Two large earthquakes have caused severe damage along the Siulak segment of the Sumatran fault. On June 3, 1909, most of the region traversed by this segment was devastated by an earthquake judged to have a magnitude of about Ms 7.7 [*Abe*, 1981]. The zone of greatest damage during the M 7.0 earthquake of October 6, 1995, was within the broad valley northwest of Lake Kerinci (Indonesian newspaper *Kompas*, October 7, 1995).

2.3.9. Suliti segment (1.75°S to 1.0°S). This 95-km-long segment has a comparatively straight fault trace, which terminates on both the northwest and southeast at dilatational step overs within volcanic edifices (Figure 4 and Plate 1). The northwestern step over, at Lake Diatas and Talang volcano, is 4 km wide. The details of the central reaches of the segment are obscure because the fault traverses the narrow valley of the Suliti River headwaters for more than 50 km. How much of this course of the fault along the Suliti River valley represents a dextral offset is unknown because the trunk stream does not cross the fault. Along the southernmost part of this segment, tributaries of the Liki River are offset several hundred meters.

The first of two large earthquakes of June 9, 1943 (M_s 7.1 [*Pacheco and Sykes*, 1992]), may have involved rupture of the northern part of the Suliti segment, judging from serious damage to Muaralabuh village, 25 km northwest of southeastern terminus of the segment [*Natawidjaja et al.*, 1995].

2.3.10. Sumani segment (1.0°S to 0.5°S). This 60-km-long segment runs northwestward from the volcanic terrane of Lake Diatas to the southwestern flank of Lake Singkarak, which occupies a structural graben, rather than a volcanic caldera (Figure 4 and Plate 1). Two opposing arcuate normal oblique faults form topographic scarps that rise 400 m above the surface of the lake (Plate 3). Ancient upland surfaces, with drainages flowing away from the lake, are clearly truncated by the steep scarps bounding the lake basin and thus appear to have been faulted down below the waters of the lake.

Failure of the Sumani segment produced the second of two large earthquakes (Ms 7.4 [*Pacheco and Sykes*, 1992]) on June 9, 1943 [*Natawidjaja et al.*, 1995]. Shaking intensities indicate that the northwestern end of the fault rupture was beneath the lake. Eyewitness accounts led *Untung et al.* [1985] to conclude that right-lateral offsets of up to 2 m occurred near the town of Solok, but *Natawidjaja et al.* [1995] could only verify offsets of ~1 m. Analysis of geodetic data supports a meter or so of dextral slip [*Prawirodirdjo et al.*, this issue].

High intensities in the vicinity of Lakes Dibawah and Diatas suggest that the entire southeastern part of the segment also ruptured, and perhaps even the northwestern part of the Suliti segment.

The first of two large earthquakes on August 4, 1926 was most severe in the narrow zone along the Sumani segment. Another earthquake, on October 1, 1822, was most severe between the Marapi and Talang volcanoes (Wichman, as cited by *Visser* [1927]). Thus this earthquake may well have involved rupture of the Sumani segment. *Genrich et al.* [this issue] show that strain accumulation during the early to mid-1990s is consistent with 23 ± 5 mm/yr of dextral slip on this segment.

2.3.11. Sianok segment (0.7°S to about 0.1°N). This predominantly straight and continuous segment runs ~90 km from the northeast shore of Lake Singkarak, along the southwest flank of the great stratovolcano Marapi to a 10-km-wide right step over at the equator (Plate 1 and Figure 4). Its southern 18 km, on the flank of Lake Singkarak, is arcuate and must have a significant component of normal faulting down toward the lake. Geomorphic expression of the fault is particularly interesting along the Sianok segment because it traverses the flank of Marapi volcano and the young, 200-m-thick pyroclastic flow deposit of Maninjou volcano. Stream channels flowing off Marapi display clear dextral offsets that range from ~120 to 600 m. The trunk channel of the Sianok River is incised into the Maninjou Tuff and display offsets of ~700 m (Figure 3). We have been able to use these offsets to determine a dextral rate of slip of ~11 mm/yr (D. Natawidjaja and K. Sieh, manuscript in preparation,2000).

The second of two large earthquakes on August 4, 1926, was most severe along the southeastern portion of the Sianok segment. This is consistent with *Visser's* [1927] observation of fault rupture between Bukittinggi and Singkarak. *Genrich et al.* [this issue] show that strain accumulation across this segment in the early to mid-1990s is consistent with dextral slip of 23 ± 3 mm/yr.

2.3.12. Sumpur segment (equator to 0.3°N). Data along this 30-km-long segment and its northwestern neighbor are scant. Our map is based predominantly upon 1:250,000-scale

Plate 2. Shaded-relief map of the Sumatran fault where it crosses the western flank of a highly dissected volcano at about 4.2°S. Colored arrows mark several offsets of the Air Kiri and Air Kanan ("river left" and "river right") of ~2.4 km. Created from 1:50,000-scale topographic map.

geologic maps [*Rock et al.*, 1983, *Aspden et al.*, 1982] and poorly reproduced 1:50,000-scale topographic maps.

Both termini of the Sumpur segment are at large dilatational steps. Thus, between the Sianok and Barumun segments, the fault experiences a 35-km-wide, double-dilatational step over. The northwestern step is associated with a high west facing escarpment and the adjoining wide valley of the Sumpur-Rokan River.

2.3.13. Barumun segment (0.3°N to 1.2°N). This 115-km-long segment is broadly concave toward the southwest and forms most of the northeastern leg of the Equatorial Bifurcation (Figure 4 and Plate 1). The southeastern 40 km of the Barumun segment forms the boundary between a high west facing escarpment and the broad depression of the Sumpur River. We interpret this escarpment and adjacent depression to be evidence of a significant component of extensional dip slip on this portion of the Barumun segment. We place the northwestern end of the Barumun segment somewhat arbitrarily at an abrupt 15° bend in the trace of the fault, near the headwaters of the Barumun River.

Only along its northernmost 35 km have we been able to inspect 1:100,000-scale aerial photography. There the fault traces display clear geomorphic evidence of strike slip. The channel of the Barumun River may be offset about 20 km, but this offset is not compelling because the trunk stream does not cross the fault.

2.3.14. Angkola segment (0.3°N to 1.8°N). The southwestern branch of the Equatorial Bifurcation consists of a continuous fault with an abrupt 30° bend at about 0.65°N (Figure 4 and Plate 1). Geomorphic expression is particularly clear between about 0.8°N and 0.5°N. *Katili and Hehuwat* [1967] used offsets of tributaries to the Angkola River at about 0.55°N to demonstrate right-lateral offsets ranging from 200 to 1200 m along this segment. The northern 30 km of the Angkola segment consists of a set of discontinuous faults on the southwestern flank of the Sarulla graben. Although large-scale aerial photographs do show minor, discontinuous faulting at about 0.35°N, the lack of through going geomorphic expression of the western branch south of 0.5°N shows that the fault is significantly less active there. The western segment does not rejoin the northeastern strand just north of the Equator. Geologic mapping supports this interpretation, and suggests that total slip on the western branch cannot be large [*Rock et al.*, 1983]. Geodetic measurements spanning the early to mid-1990s suggest that modern strain rates are higher in the vicinity of the Angkola segment than on the main segment farther east [*Genrich et al.*, this issue]. Combined slip at depth at a rate of 23 ± 4 mm/yr satisfies the geodetic measurements.

The Angkola segment of the Sumatran fault produced the famous earthquake of 1892, during the establishment of the first primary triangulation network in the region. Differences in angles measured just before and after the earthquake enabled *Müller* [1895] to calculate that coseismic right-lateral dislocations of at least 2 m had occurred along a northwest trending line coincident with that portion of the fault trace between 0.45°N and 1.2°N. These geodetic data, along with those from the 1906 San Francisco earthquake and 1891 Mino-Owari earthquake inspired, *Reid* [1913] to formulate the theory of elastic rebound [*Yeats et al.*, 1997, Chapter 8]. *Prawirodirdjo et al.* [this issue] have reanalyzed the Dutch data and conclude that the dextral slip was 4.5 ± 0.6 m. The most serious damage reported in 1892 was along the fault in the valleys of the Gadis and Angkola Rivers, between Malintang and Lubuk Raya volcanoes [*Visser*, 1922].

2.3.15. Toru segment (1.2°N to 2.0°N). Major bends in the fault trace delimit this segment of the Sumatran fault (Figure 4 and Plate 1). We define the southern terminus to be at a regional bend of 15° at 1.2°N. The topographic high east of the bend suggests that this is a contractional bend.

The northwestern termination of the Toru segment occurs at a 15° regional bend in the fault, which is coincident with a 2.5-km dilatational step over. We can be confident that this bend is dilatational because the segment to the northwest does not display net vertical deformation across the fault and the bend coincides with the Tarutung depression.

Northwest of Sibual-buali volcano, a 30-km-wide caldera northeast of the fault is truncated by the fault. The other half of the caldera, southwest of the fault, must be concealed beneath young volcanic deposits. The geomorphic expression of the fault in the vicinity of the truncated caldera is unusually complex. Significant components of dip slip occur on faults that splay northward from the main trace into the caldera. The Toru segment has not produced a major historical earthquake, but right-lateral slip near the northern end of this segment did generate the M_s 6.4 Pahae Jahe earthquake of 1984.

2.3.16. Renun segment (2.0°N to 3.55°N). This longest segment of the Sumatran fault traverses the western flank of the 80-km-long Toba caldera, alleged to be the largest Quaternary caldera on Earth [*Chesner et al.*, 1991]. Much of the Renun segment traverses the thick pyroclastic flow deposit of that 73,000-year-old eruption. The regional expression of this 225-km-long segment is linear, except for a dogleg along its northwesternmost 30 km, where the segment forms the southwestern flank of the Alas Valley graben. This graben, 45 km long and 9 km wide, is one of the largest graben along the Sumatran fault. West of Lake Toba, the fault consists of several 30- to 40-km-long strands, arranged en echelon, with across-strike separations of only a kilometer or so. Although the right-stepping nature of the en echelon pattern suggests that the fault is experiencing a minor component of transtension in the upper crust, the step overs are associated with horsts, not graben.

The southeasternmost part of the Renun segment exhibits a well-defined 2-km offset of the 73,000-year-old Toba Tuff, which we have used to determine a 27 mm/yr slip rate for the fault [*Sieh et al.*, 1991; D. Natawidjaja and K. Sieh, manuscript in preparation, 2000]. GPS measurements across the southern portion of this segment suggest slip rates of 24 ± 1 mm/yr below ~9 km. Across the northern portion of the Renun segment, geodetic rates appear to be 26 ± 2 mm/yr [*Genrich et al.*, this issue].

The Renun segment was the source of three major earthquakes early in the twentieth century. Accounts of these events are very sparse, however, and the limits of the rupture can only be guessed from poorly constrained isoseismal contours. *Visser* [1922] reports that shaking during the February 22, 1916, earthquake was very strong in the Tarutung valley and that the radius of strong shaking was ~200 km. The January 24, 1921, earthquake had a region of severe shaking similar to that of the earthquake of 1916. The radius of shaking for the earthquake of April 1, 1921, was twice as large [*Visser*, 1922].

2.3.17. Tripa segment (3.2°N to 4.4°N). Marked irregularity and curvature, mountainous terrain, and

spectacular dextral offsets of major rivers characterize this 180-km-long segment (Figure 4 and Plate 1). The location of the main trace of the fault is well constrained by spectacular offsets of the Kuala Tripa and Meureubo Rivers. Each of these deeply entrenched rivers displays a clear offset of ~21 km (Figures 6 and 7 and Tables 2 and 3).

The segment's southeastern terminus is the northeastern flank of the extensional Alas Valley graben. Its northwestern limit is a 9-km-wide restraining bend, which displays south-side-up faults with a significant component of reverse slip. One could argue that an appreciable contractional jog at 4.0°N and a major change in strike at 3.85°N justify dividing this segment further.

Parallel to and ~15 km northeast of the central portion of this segment (between 4.0° and 4.25°N) is another active strike-slip fault. This 55-km-long fault trace is also well defined by aligned river valleys and stream offsets. Stream patterns suggest that this fault may converge with the main active trace at the northwestern terminus of the Tripa segment. However, we could find no clear large-scale geomorphic evidence of this, nor does the 1:250,000-scale geologic mapping suggest it [*Cameron et al.*, 1983].

An earthquake on September 19, 1936, occurred along the southeasternmost part of the Tripa segment (M_s 7.2 [*Newcomb and McCann*, 1987]). A smaller, more recent shock (m_b 6.0, November 15, 1990) occurred near the middle of this segment.

2.3.18. Aceh segment (4.4°N to 5.4°N). This 200-km-long segment of the Sumatran fault has a smooth sinusoidal shape and lacks major discontinuities or sharp bends (Figure 4 and Plate 1). The southeastern two thirds traverse mountainous terrain and are well expressed by aligned major river canyons and stream offsets. Dextral separations of ~25 and 20 km on the Geumpang and Woyla River channels are not compelling evidence for offset, but they are similar in magnitude to the size of clear offsets of the Tripa and Meureubo Rivers farther southeast (Figure 7). The northwestern portion of the Aceh segment traverses a region of low relief and is obscure on 1:100,000-scale aerial photographs. Geomorphic expression of the fault is subtle and stream offsets appear to be absent there. Although some published maps show the Sumatran fault running along the southwestern flank of the Aceh Valley and continuing into the sea across the northwestern coast [*Curray et al.*, 1979; *Page et al.*, 1979], we see no geomorphic evidence of active faulting within 25 km of the coastline. Therefore, we, are not convinced that the fault is active northwest of about 5.4°N. Geomorphic evidence for inactivity is compatible with geodetic observations that strain is accumulating at no more than a few millimeters per year across the fault [*Genrich et al.*, this issue].

2.3.19. Seulimeum segment (5.0°N to 5.9°N). This segment represents the principal active trace of the Sumatran fault through northern Aceh province (Figure 4 and Plate 1). The active trace is marked by sharp escarpments and dissected young volcanic deposits on the southwestern flank of Seulawah Agam volcano. Small tributaries of the Seulimeum River are clearly offset a few hundred meters. Along the central part of this segment, young folds appear to be offset ~20 km (Figures 6 and 7 and Tables 2 and 3).

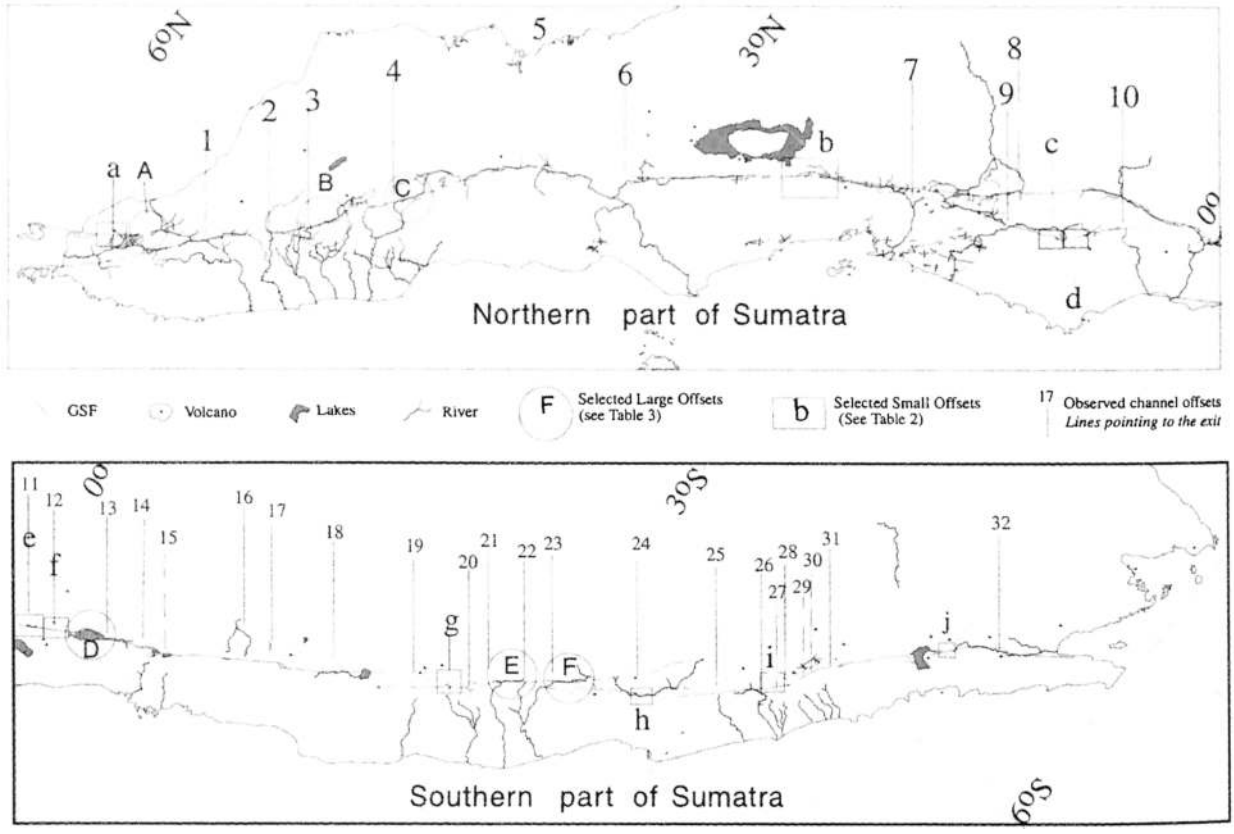

Figure 6. Map of small and large geomorphic offsets along the Sumatran fault. See Tables 2 and 3 for more information. The largest offsets indicate that total slip across the fault is at least 20 km.

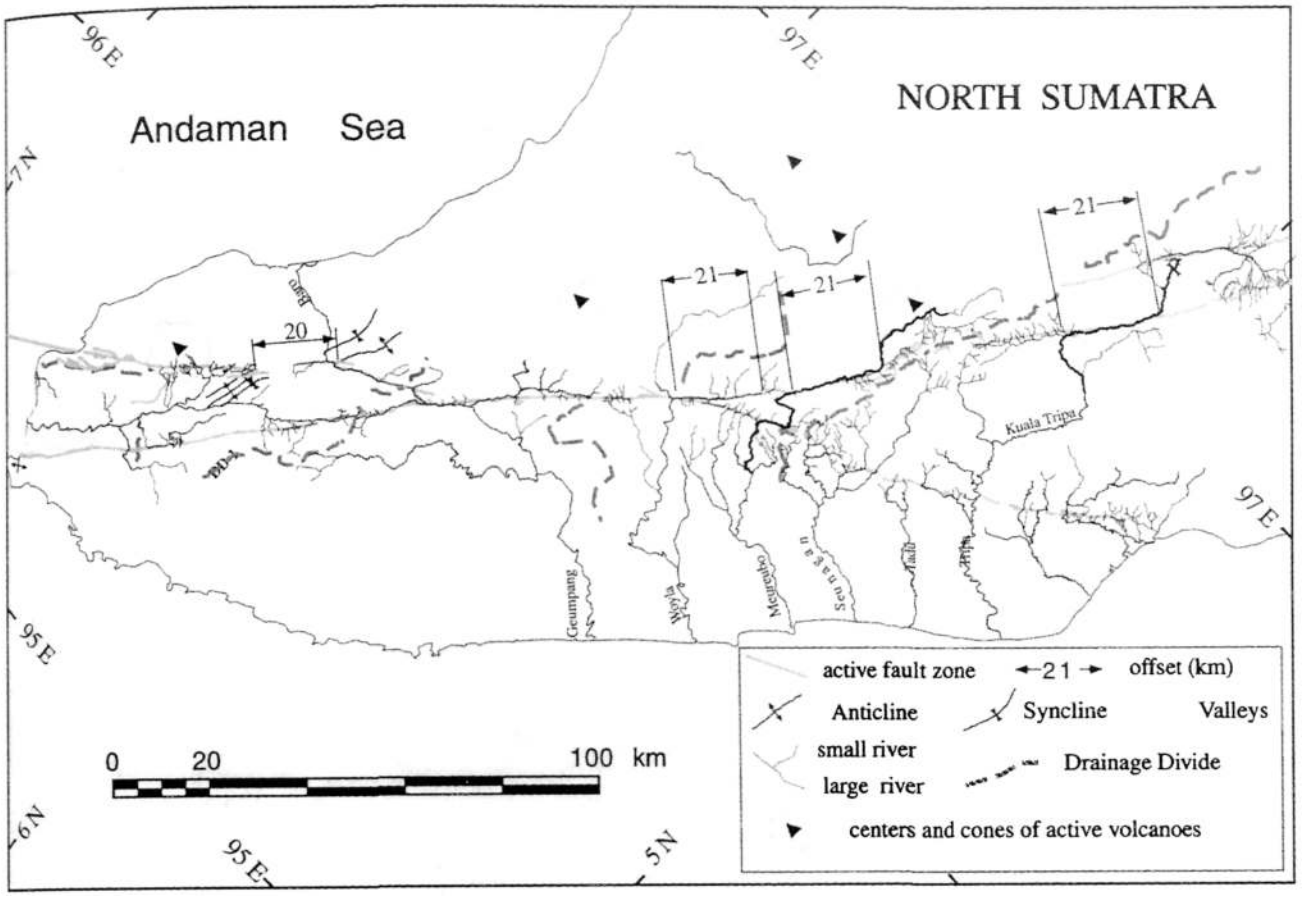

Figure 7. Two of the most compelling large geomorphic offsets along the Sumatran fault, the 21-km dextral offsets of the Tripa and Meureubo Rivers in north Sumatra. The headwaters of the nearby Woyla River and folded Quaternary sediments near 6°N also appear to be offset by this amount. These offsets appear to represent the total dextral offset since initial uplift of this part of the Barisan Mountains several million years ago.

Clear evidence of recent activity along the southeastern 22 km of this segment is absent from our aerial photos, but we infer that the fault continues through the long, narrow valley of the Baro River along this reach to an intersection with the Aceh segment at about 5°N. Northwest from the coastline, bathymetry [*Curray et al.*, 1979; J. Curray, written communication, 1999], focal mechanisms (Harvard CMT catalogue), geomorphic expression of faulting on Weh Island, and evidence on a seismic reflection profile [*Peter et al.*, 1966; *Weeks et al.*, 1967] suggest that the fault continues under water.

It is interesting that dextral movement along the Seulimeum segment has produced no deflection of the Aceh segment at their intersection. It is difficult to imagine how many kilometers of dextral slip on the Seulimeum segment could have occurred without at least a broad deflection in the Aceh segment.

A large earthquake in 1936 (M 7.1-7.3 [*Newcomb and McCann*, 1987; *Soetardjo et al.*, 1985]) severely damaged the city of Banda Aceh, but the source of the event is unknown. An earthquake in 1964 (M_s 6.5, National Earthquake Information Center (NEIC)) damaged Krueng Raya more severely than Banda Aceh. Since Krueng Raya is closer to the Seulimeum segment, the Seulimeum segment of the Sumatran fault may have generated this event. In contrast to the geomorphic evidence for recent dextral slip along the Seulimeum segment, *Genrich et al.* [this issue] show that strain accumulation across this segment in the early 1990s could be nil.

2.4. Other Related Structures

2.4.1. Batee fault. The Batee fault is a major right-lateral strike-slip fault that diverges from the Sumatran fault at about 4.65°N. Between its intersection with the Sumatran fault and the coastline, the fault traverses the 1000-m-high southwestern escarpment of the Barisan range. *Karig et al.* [1980] have shown that this structure continues onto the continental shelf and offsets the edge of the continental shelf ~150 km and the eastern edge of the outer-arc ridge ~100 km. One strand of the Batee fault terminates before reaching the northern part of Nias Island (Plate 1). Another strand runs along the northern coast of Nias and appears to offset the inner trench slope and outer-arc ridge (Plate 1). Except very locally, the Batee fault does not appear to be active on the mainland of Sumatra. Although several large river channels display dextral deflections of up to 10 km, smaller ridge lines and channels exhibit no offset. We suspect that these large deflections are, indeed, dextral offsets, but the lack of clear small offsets suggests either no activity in the past few tens of

Table 2. Selected Small Offsets Along the Sumatran Fault (From North to South)

	River/Lake Name	Offset, m	Comments
a	Aceh River	750-1000	offset of several streams that incised young volcanic deposits on the southwest flank of Seulawah Agam volcano
b	Toru River	1700-2100	excellent offset of several streams deeply cut into the 73,000 year old Toba Tuff
c	Angkola River	1200-1400	offsets of a few streams on the northeast flank of the Sorik Merapi volcano
d	Angkola River (Ringkit branch)	1000-1300	offsets of several tributaries of the Angkola River
e	Sianok River	700	excellent offsets of several crossings of the Sianok River, deeply incised into the 60,000 year old Maninjau Tuff
f	Anai River	600	offsets of several channels on the southwest flank of Merapi volcano
g	Lake Dipatiampat	500	offset of north sidewall of the caldera lake
h	Musi River	700	excellent offsets of tributaries to the Musi River, on the southwest flank of Kaba volcano
i	Manna River	2400	offset of Air Kiri and Air Kanan (Plate 2) which drains an eroded volcanic edifice
j	Werkuk River (Menjadi, Pisai, Rebu branches)	300	offsets of three channels that are deeply incised into the thick, Quaternary Ranau Tuff

thousands of years or activity at a rate much lower than along the Sumatran fault. This interpretation conflicts with the 12 ± 5 mm/yr estimate of dextral slip rate of *Bellier and Sebrier* [1995]. We question the validity of their approach, which uses an empirical relationship of channel length and age to derive an age for a channel. This age is then divided into the measured offset to determine a rate.

2.4.2. Toru fold and thrust belt. Between about 1.0° and 1.5°N lies a geomorphologically remarkable set of active folds and faults that strike roughly parallel to the Sumatran fault but lie 15 to 40 km farther southwest (Plate 1). The principal manifestations of this fold-and-thrust belt are a northwest striking anticline and syncline. The syncline underlies a 25-by-10-km swamp, and the anticline appears as a 30-by-15 km fold in Mio-Pliocene sediment. The Gadis River and its tributaries meander across the syncline and then traverse the anticline as an antecedent stream.

In addition, several smaller northwest striking reverse faults appear to break the anticline (Plate 1). The anticline also is cut by small north striking strike-slip faults. However, these faults are so small and closely spaced that they do not appear on Plate 1.

3. Discussion, Interpretations, and Speculations

In this paper, we have defined the geometry and geomorphology of the Sumatran fault. There are now several questions that these refinements allow us to address. These include the implications of the fault's historic behavior and geometry for the evaluation of future seismic hazard and questions about the total offset across the Sumatran fault and its role in oblique convergence during the past many millions of years. Other questions concern the geometric and kinematic relationship of the Sumatran fault to the neighboring subduction zone and the relationship of arc volcanism to strike-slip faulting. We address each of these four questions in turn, below.

3.1. Historical and Future Seismicity

In the preceding discussion, we have described very briefly what is known about large earthquakes along the Sumatran fault. Even these highly abbreviated accounts suggest that geometric segmentation influences seismic rupture of the Sumatran fault. In contrast to the San Andreas fault in California [*Lawson et al.*, 1908; *Sieh*, 1978], the Sumatran

Table 3. Proposed Large Offsets Across the Sumatran Fault

	Features	Offset, km	Quality	Description
A	Quaternary folds	20	fairly good	offset of a few fold axes which deformed Pliocene, Miocene, and Oligocene strata
B	Meureubo River	21	excellent	dextral offset is clearly indicated by the deflection of the trunk channel
C	Tripa River	21	excellent	dextral offset is clearly indicated by the deflection of the trunk channel
D	Singkarak graben	20-22	N/A	based on an interpretation of the graben opening (Figure 7)
E	Seblat River	17	good	clearly shown by a sharp deflection of the main channel
F	Ketahun River	23	good	clearly shown by a sharp deflection of the main channel

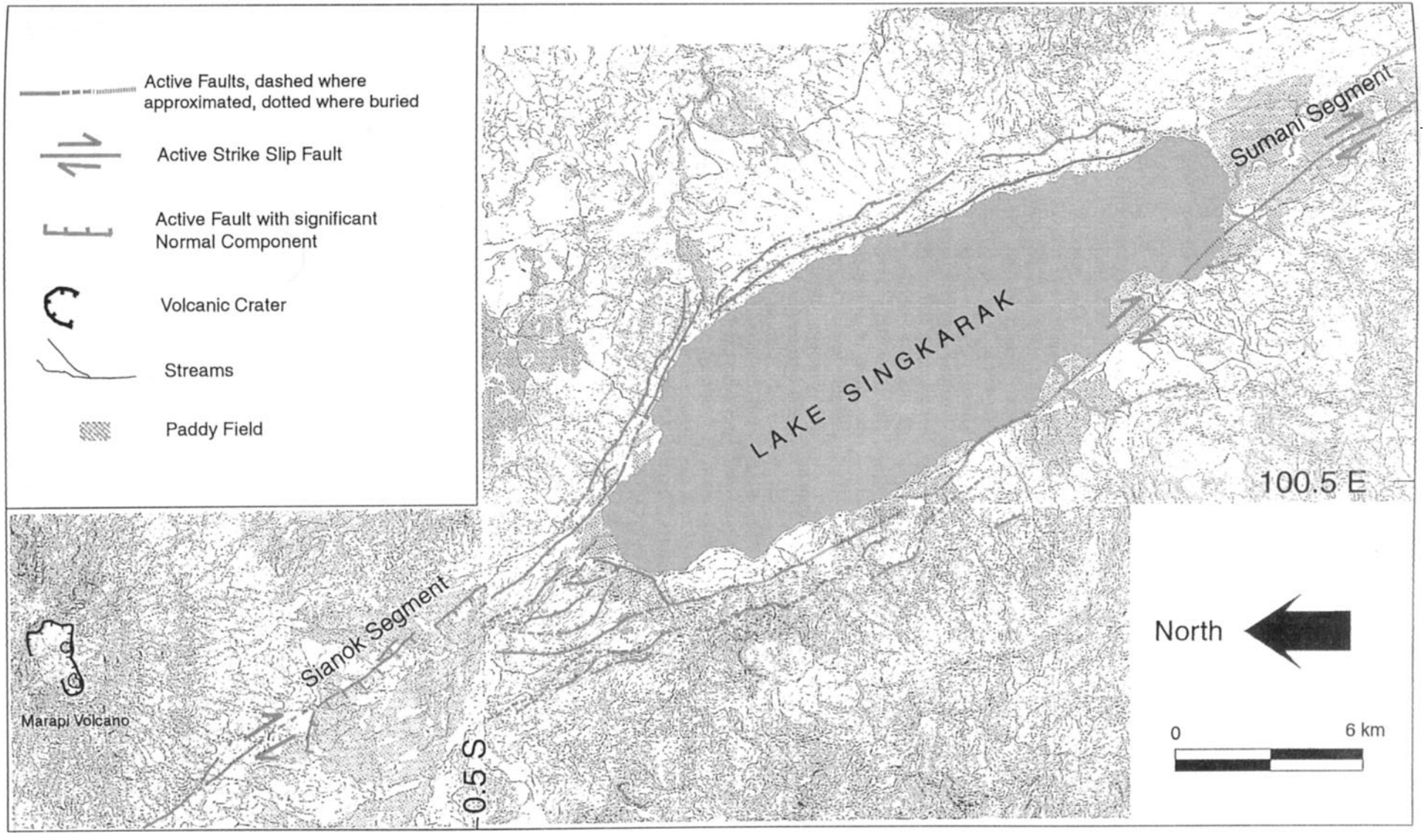

Plate 3. Map of the Sumani and Sianok segments near the Singkarak graben. The youthful appearance of the bounding normal faults suggests that accommodation space continues to form as the en echelon Sumani and Sianok segments accumulate dextral slip. Topography is from 1:50,000-scale quadrangles. The fault geometry was compiled from the topographic maps and stereo aerial photographs.

fault appears to produce earthquakes with rupture lengths no greater than a hundred kilometers or so. We speculate that this contrast in behavior results from the contrast in continuity of the two fault systems: The San Andreas fault has only one step over discontinuity with a cross-strike width greater than a kilometer (near San Gorgonio Pass [*Allen*, 1957]), whereas the Sumatran fault has at least 12. The San Andreas has only two large bends (near Monterey Bay and at Tejon Pass) [*Jennings and Saucedo*, 1994], whereas the Sumatran fault has about eight.

A more precise and detailed evaluation of the relationship of these irregularities and their relationship to historical ruptures is warranted but is beyond the scope of this paper. We have begun a thorough analysis of the historical accounts and hope to interest a seismologist in studying instrumental records in order to assess more fully the role of geometric segmentation in controlling rupture parameters. Until this future work is completed, one can obtain a crude sense of the influence of fault segments on historical ruptures by comparing *Katili and Hehuwat's* [1967] compilation of the felt regions of historical earthquakes with our map of the fault. *Bellier et al.* [1997] have redrawn Katili and Hehuwat's map and include a few more recent earthquakes in their compilation of historical felt areas.

3.2. Offsets Across the Sumatran Fault and the Evolution of Dextral Slip Along the Sumatran Margin

3.2.1. Exemplary small to moderate offsets. None of the geomorphic offsets across the Sumatran fault are greater than ~20 km, and most are far smaller (Figure 6 and Tables 2 and 3). The smallest known offsets along the Sumatran fault are those associated with particular historic fault ruptures. These include offsets of a meter or two on the Sumani segment (0.75°S), during the 1943 earthquake [*Untung et al.*, 1985] and up to about 4.5 m during the 1892 earthquake, on the Angkola segment (about 0.6°N) [*Müller*, 1895; Reid, 1913; *Prawirodirdjo et al.*, this issue]. Our best examples of dextral offsets in the range of hundreds of meters to a couple kilometers are on or near the flanks of young volcanoes: Channels on the southwest flank of Kaba volcano (3.6°S) are offset ~700 m. The walls of Dipatiampat caldera (2.65°S) are offset ~500 m. Stream channels incised into the southwest flank of Marapi volcano display offsets ranging from 120 to 600 m. The Maninjou Tuff (0.4°S) has been offset 700 m (Figure 3), and channels cut into the Toba Tuff (2.2°N) are offset about 2 km (Table 2). We have used three of these to determine the modern slip rate of the Sumatran fault, but full documentation of these rates is the subject of a manuscript in preparation.

As one would expect, highly dissected volcanic landforms are offset more than their younger neighbors are. The two offset streams cutting a dissected volcanic edifice at 4.2°S are good examples of this. They are offset about 2.5 km (Plate 2).

3.2.2. Largest geomorphic offsets. The largest plausible geomorphic offsets along the Sumatran fault are ~20 km (Table 3, Figures 6 and 7, and Plate 1). These include right-lateral deflection of the channels of the Ketaun River channel at 3.2°S, the Seblat River channel at 2.9°S, and the Tripa and Meureubu River courses at 4.1° and 4.4°N (Plate 1). Late Cenozoic folds at 5.25°N may also be offset ~20 km. Furthermore, we speculate below that the Singkarak graben (at 0.6°S) has developed in response to 23 km of offset.

The two major offsets between 5° and 5.5°N provide the most compelling evidence from stream channels for large offset along the Sumatran fault (Figure 7). The deeply incised trunk channels of both streams cross the fault at a high angle and have long, straight courses along the fault trace. The neighboring Woyla River drainage also appears to be offset ~21 km, but this offset is less certain because the match across the fault is of trunk channel to tributary channels. The drainage divide between the Woyla and Geumpang Rivers also appears to be offset by ~20 km.

One could propose 40- to 50-km offsets for the deeply entrenched channels of the Tripa and Meureubo Rivers, but this would leave implausible mismatches in the surrounding topography. Our proposed 20- to 30-km offset of an anticline/syncline pair at about 6.4°N, which is based upon a plausible offset of folded Pliocene, Miocene, and Oligocene rocks [*Bennett et al.*, 1981] (Figure 7), supports the interpreted 20-21 km offset of the Tripa and Meureubo Rivers.

Another large offset that we will consider in more detail is one we can infer from the geometry of the normal faults along the Singkarak graben at about 1.4°S. This is more speculative than the geomorphic offsets described above. In most cases, the length of a pull-apart graben along a strike-slip fault probably does not represent the total slip across the fault zone (for example, the 7-km-long step over mapped by *Zachariasen and Sieh* [1995] between two faults in California has only 300 m of total offset across it). The particular nature of the faults bounding the Singkarak graben suggests that it may be an exception.

Although the dextral fault segments coming into the step over from the northwest and southeast are misaligned by only ~3.5 km, the normal faults bounding the lake are separated by as much as 7.5 km (Plates 1 and 3). Because of their salad-tong geometry, we surmise that the normal faults represent collapse of shallow crust into the expanding rectangular region that is being produced by dextral slip on the misaligned lateral faults.

The predominance of volcanic rocks of Plio-Pleistocene age on the flanks of the graben indicate that the graben is no more than a few million years old. *Bellier and Sebrier* [1994] proposed that the Singkarak basin is an extinct pull-apart graben, inactivated when the trace of the Sumatran fault cut across the lake. The very steep scarps and youthful topography associated with the graben-bounding normal faults strongly suggest, however, that accommodation space continues to be created by dextral slip on the en echelon Sumani and Sianok segments. Furthermore, the location of the 1943 rupture is inconsistent with a competing model for the evolution of the fault by *Bellier and Sebrier* [1994].

We hypothesize that the normal faults should only be active adjacent to foundering crust within the accommodation space generated by dextral slip along the en echelon faults. A hypothetical evolution of these normal faults as the strike-slip displacement grew is depicted in Figure 8. Therefore, we propose, that the total offset on these two misaligned strike-slip segments is ~23 km, the length of the arcuate normal fault zones on either side of the lake.

This is, of course, not the only plausible evolution for the Singkarak pull-apart graben, but it is one that is consistent with ~20 km of total offset along the Sumatran fault. One could, for example, accept our inference that the lengths of the normal faults reflect the fault-parallel length of actively

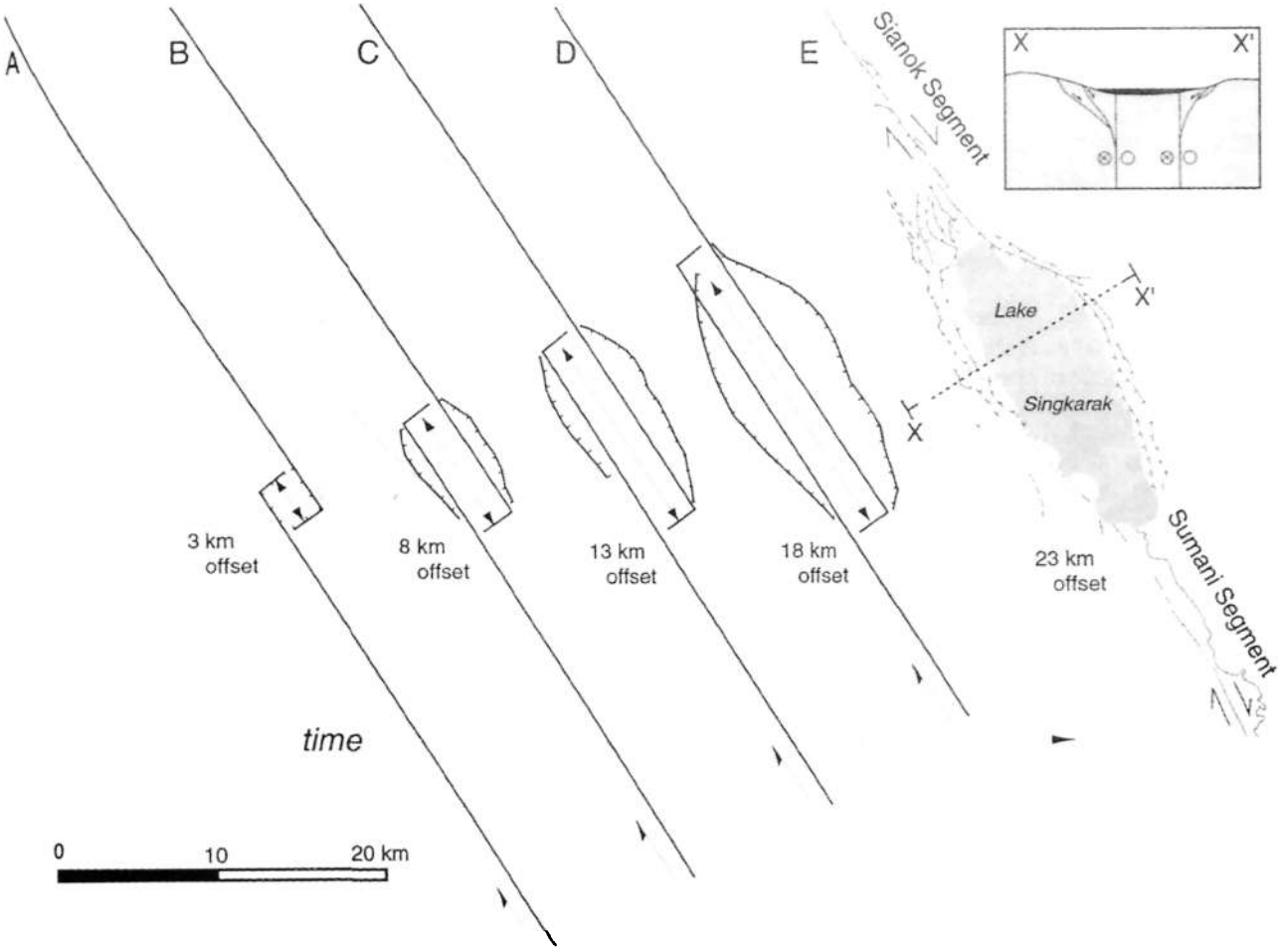

Figure 8. Hypothetical evolution of the Singkarak graben and bounding normal faults showing how the length of the normal-oblique faults might represent the total offset on the Sianok and Sumani segments. Profile E shows the current geometry of the graben.

foundering crust but hypothesize that the length of the foundering region has remained unchanged at ~23 km since the faults initiated. This would imply that the length of the foundering region has no bearing on the amount of total offset. We favor our hypothesis because it is consistent with other evidence for ~20 km of total offset.

3.2.3. Total offset. Why are the largest geomorphic offsets no greater than ~20 km? Is it possible that these represent total strike-slip offset along the Sumatran fault? Or is there a limit to the size of geomorphic offsets related to the susceptibility of landforms to erosion and burial? We will give reasons below why 20 km might well be the total offset across the fault, but we will also show that a total offset as great as ~100 km can not be ruled out at this time.

Indirect arguments for offset much greater than 20 km are as follows: One might expect that the great length of the Sumatran fault requires substantially greater total offsets than a couple tens of kilometers. It is certainly true that many very long strike-slip faults, such as the Alpine (New Zealand) and San Andreas (California) and many oceanic ridge-ridge transform faults display geologic offsets of hundreds of kilometers [*Yeats et al.*, 1997, Chapter 8].

But this is not a strong argument for large offset, for two reasons. First, many other very long strike-slip faults have accrued only a few tens of kilometers of offset. An example is Turkey's 1500-km-long North Anatolian fault, which has a total offset of only 85 km [*Armijo et al.*, 1999]. Second, in a strict sense, the Sumatra fault is not one fault; rather, it is a fault zone that consists of many segments, which range in length from 60 to 220 km. Many strike-slip faults with lengths as short as these have accrued only a few kilometers to a few tens of kilometers of offset (for example, the San Jacinto fault in California is a zone with 24 km of dextral offset that consists of many disjunct segments, tens of kilometers long).

Another reason to suspect that total slip would be >20 km is the transformation of the Sumatran fault into the spreading centers of the Andaman Sea [*Curray et al.*, 1979]. This suggests that offset could equal the 460 km of spreading that has occurred there in the past 10 Myr. But we will see below that much of this offset has been carried by faults that splay into the forearc, west of the Sumatran fault zone.

Regardless of plausible analogues and the fault's connection to the spreading centers of the Andaman Sea, direct geologic evidence for total offset across the Sumatran fault is sparse and equivocal. *McCarthy and Elders* [1997] suggest 150 km of dextral slip, on the basis of similarities in isolated outcrops of crystalline basement on both sides of the

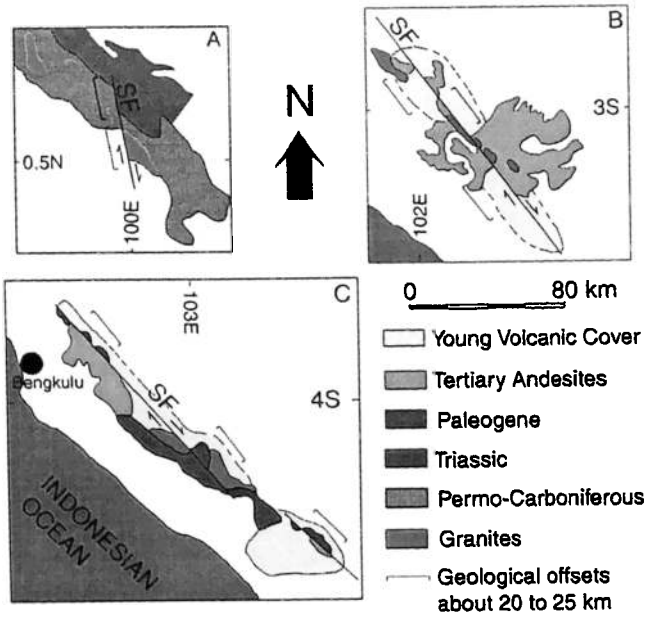

Plate 4. Geologic maps of offset bedrock units along three sections of the Sumatran fault suggesting that the total offset across the fault is only ~20 km. Reproduced from *Katili and Hehuwat* [1967].

fault in central Sumatra. *Katili and Hehuwat* [1967], however, infer that total dextral offset at three localities (near the equator, 3°S, and 4°S) is only 20 to 25 km on the basis of regional-scale maps of late Paleozoic to early Cenozoic rocks (Plate 4). *Cameron et al.* [1983] suggest a 20-km dextral offset of Oligocene beds at about 4.1°N. Neither the larger nor the smaller offsets are adequately defended by sufficiently detailed mapping.

The geologic setting of the Sumatran fault supports the notion that geomorphic offsets might be limited to less than a few tens of kilometers and that these values could be significantly less than the total offset. The abundance of young volcanic cover, the spacing of major river channels, and the length of individual fault segments all limit the accumulation of geomorphically evident offset. Let us consider volcanic cover first. More than a quarter (~450 km) of the 1650-km-long Sumatran fault traverses young volcanic edifices and their thick pyroclastic deposits. Most or all of these volcanic constructions are probably far less than a half million years old, given their generally undissected nature. Even if the Sumatran fault carried all the dextral component of the relative plate motion vector (~30 mm/yr), no more than ~15 km of offset could have accumulated since their deposition. Burial of older offsets would have obscured or eliminated their clear geomorphic expression.

Clear geomorphic offsets are also limited by the length of individual fault segments, which range in length from ~35 to 220 km (Table 1). Since the majority of the fault segments are right-stepping, graben are common along the fault. These graben form intramontane valleys that occupy about ~350 km of the fault. As these basins form, streams divert into them. The Alas graben, between 3.1° and 3.9°N, has probably enabled such a diversion. The Alas River drains a 130-km reach of the fault into the 50-km-long graben before breaching the graben wall and flowing southwestward to the Indian Ocean. The flow of the Sumpur River, between about 0.1° and 0.75°N, has also been strongly influenced by subsidence along the fault; major tributaries flow into and across the Sumpur Valley before flowing eastward toward the Java Sea from their confluence at the fault.

A third limit to the size of geomorphic offsets is imposed by the spacing of major drainage channels that cross the fault. Cumulative offsets are unlikely to be greater than the spacing between major river channels because piracy occurs as trunk channels of one drainage system are offset to positions upstream from neighboring trunk channels [see, e.g., *Prentice*, 1988; *Allen et al.*, 1984; *Yeats et al.*, 1997, Chapter 8]. Along only a small percentage of the Sumatran fault are major stream channels spaced more than a couple tens of kilometers apart (Plate 1). Piracy of the headwaters of the Alasijani River by the Manna River, for example, may have occurred at about 4.1°S (Plate 1). Furthermore, where the Sumatran drainage divide is within just a couple kilometers of the Sumatran fault, large trunk stream channels do not cross the fault trace. In these places, the Sumatran fault traverses only smaller tributary drainages. Because tributaries are more closely spaced, geomorphic interference will result where offsets exceed a few kilometers. Thus only about half of the Sumatran fault might be expected to express offsets greater than a few kilometers.

Nonetheless, there is reason to favor the hypothesis that the largest geomorphic offsets are, in fact, the total offset across the fault. The 20- to 21-km offsets of deeply incised channels in northern Sumatra probably record total offset since the initiation of uplift of the Barisan mountain range in this region, and that uplift is quite old. The age of initiation of uplift is poorly constrained, but sedimentation history of the forearc basin suggests that Sumatran sediment sources began eroding in late mid-Miocene time (about 10 Ma) [*Karig et al.*, 1979; *Harbury and Kalagher*, 1991], and *Cameron et al.* [1980] document major activity of a range-bounding fault about 10 Ma. If this is true, then incision of the Tripa and Meureubo Rivers would also have begun about 10 Ma, and the 21-km offsets would necessarily reflect total offset since that time. The nearby 20-km offset of an Oligocene sedimentary unit proposed by Cameron et al. [1983] suggests that this may be the total offset since the Oligocene as well. Our analysis of the Singkarak graben also suggests that 23 km is the total offset across the Sumatran fault since formation of the two bounding faults, the Sumani and Sianok segments. If the total offset across the fault were greater, proof would require discovery of an older fault, hidden beneath the younger sediments of the region.

3.2.4. Evidence of stretching near the Sunda Strait. A simple structural analysis of the forearc region near the southern terminus of the Sumatran fault provides support for ~100 km of total offset across the Sumatran fault system. However, as we will show, not all of this, nor even a majority of it, need be associated with the Sumatran fault.

Two earlier papers discuss stretching of the forearc near the southern terminus of the fault. *Huchon and Le Pichon* [1984] were the first to suggest that arc-parallel stretching of the forearc region near the Sunda Strait is related to strike slip along the Sumatran fault. They hypothesized that the landward bend in the subduction deformation front and the absence of an outer-arc ridge and forearc basin south of the Sunda Strait (Figure 5) indicate arc-parallel stretching of the forearc region. However, they did not use this to calculate

plausible amounts of offset along the Sumatran fault. Instead, they accepted sparse and equivocal evidence for ~100 km of total offset along the fault and attempted to demonstrate that this offset is consistent with reasonable estimates of arc-parallel stretching. They did not attempt a rigorous assessment of the implications of the forearc geometry on total offset along the Sumatran fault.

Lassal et al. [1989] also attempted to quantify the stretching of the forearc region south of the Sunda Strait. They show three seismic reflection lines from a 80 x 50 km area in and on the flanks of the graben at the western entrance to the strait. They annotate these with five stratigraphic boundaries, whose geometry and ages they defend by reference to unpublished work. They claim (without discussion or argument) that an allegedly upper Miocene stratal package contains reef deposits (an indicator of shallow water). They assume an uppermost Miocene (5 Ma) age for the reefs and then use the depth of this packet of sediment to calculate the "stretching factor" since 5 Ma. This factor is described by *Le Pichon and Sibuet* [1981], who apply a stretching model of *McKenzie* [1978] to passive continental margins. The use of this model seems wholly inappropriate to us since the parameters needed to calculate stretching are mostly unknown for the Sunda Strait. *Lassal et al* [1989], conclude by asserting, without any discussion or calculation, that this stretching factor "probably explains the opening of the strait since 5 Ma ago, with a maximum displacement of 50 to 70 km along the central Sumatra fault." Their paper is, in fact, so sparse on data and documentation that its conclusions are left undefended.

We propose a simple measure of extension across the graben of the Sunda segment, which establishes a minimum amount of dextral slip on the Sumatran fault. If we assume that the faults bounding the graben dip 60°, we can calculate the horizontal extension across the faults in the direction of the Sumatran fault. We calculate a 6.5-km lower bound on extension of the graben parallel to the Sumatran fault if we assume that the 2-km height of the scarp represents vertical throw across the faults. This assumption is manifestly an underestimate of total vertical throw, since hundreds of meters of deposits within the graben are clear on the seismic reflection cross sections. Thus 6.5 km is probably several kilometers less than the actual amount of extension across the Sunda graben. Several more kilometers of dextral slip could probably also be added to total slip along the Sumatran fault if the geometry and timing of faulting farther east within the strait and buried beneath >2000 m of volcanic debris (summarized by *Huchon and Le Pichon* [1984]) were known better. In summary, extension of the Sunda graben and filled graben farther east is consistent with dextral slip of the order of 10 km along the Sumatran fault. However, more detailed stratigraphic and structural data will be necessary to calculate extension across the graben more precisely.

Let us now attempt a quantitative analysis of stretching of the forearc region, to provide a maximum limit to dextral slip on the Sumatran fault during the past few million years. This analysis simply carries the geometrical observations of *Huchon and Le Pichon* [1984] to their logical conclusion. From simple volumetric balancing of the forearc wedge, we calculate ~100 km of stretching of the forearc parallel to the Sumatran fault.

As we discussed in section 2.3.1. (Figure 5), the forearc basin and outer-arc ridge are attenuated in the region of the Sunda Strait. These two features disappear near the strait, and the deformation front bows landward. Following *Huchon and Le Pichon* [1984], we interpret this as an indication of fault-parallel stretching and fault-normal necking of the forearc region. Extensive seismic reflection studies and structural and stratigraphic information from the forearc and outer-arc regions north of the equator show that the paired forearc basin and outer-arc ridge developed throughout the Miocene epoch but grew particularly rapidly during the Pliocene epoch [*Samuel et al.*, 1997; *Samuel and Harbury*, 1996]. Thus we infer that the deformation of these features has occurred within just the past few million years.

We begin with an estimate of the boundaries of the volume that has been stretched. The concavity of the deformation front and merging of the outer-arc ridge and forearc basin suggest that the current length of the deformed region, L, is ~356 km (Figure 9). Hypocentral depths on or near the subduction interface constrain the northeast dipping base of the deformed forearc wedge. The deformation front and the base of the continental slope define the seaward and landward boundaries of the deformed region.

Using these boundaries, we calculate that the deformed crustal wedge has a volume V, of about 1.01×10^6 km^3. We assume that this volume is equal to the original, undeformed volume V_o. By further assuming that the cross-sectional areas of the current southeastern and northwestern edges of the deformed region, A and B, have not changed since deformation began, we can calculate the original arc-parallel length of the deformed region. A and B are currently 2870 and 4970 km^2:

$$L_o = 2 * V / (A + B) = 258 \text{ km}. \quad (1)$$

The total amount of northwest-southeast stretching is:

$$\Delta L = L - L_o = 356 \text{ km} - 258 \text{ km} = 98 \text{ km}. \quad (2)$$

Since the Sumatran fault forms the northeastern boundary of the forearc sliver block, we are tempted to conclude that this estimate of stretching of the forearc equals the amount of right-lateral slip along the Sumatran fault. However, in fact, this 100 km is only an upper bound on offset of the past few million years since there is another structure in the forearc region that could also have accommodated some of this stretching. The Mentawai fault [*Diament et al.*, 1992], located between the forearc basin and the outer-arc ridge (Figures 1 and 8 and Plate 1), could also have accommodated some of this motion. The linearity of this large structure suggests a significant component of strike-slip motion, but the magnitude of strike-slip motion, if any, has not been documented.

3.2.5. Plausible evolution of dextral slip along the Sumatran margin. Although knowledge of the geology of the Sumatran fault and other faults of the Sumatran fault system is incomplete, enough information exists to attempt a reconstruction of the system's deformational history over the past few million years (Figure 10). The principal constraints on this history are: (1) the magnitude and timing of the discrepancy between spreading in the Andaman Sea and stretching near the Sunda Strait; (2) a range of plausible total offsets for the Sumatran fault; (3) the timing, style, and magnitude of deformation in the Sumatran forearc region; and (4) a southeastward decrease in the current rates of slip along the Sumatran fault. These constraints suggest that the

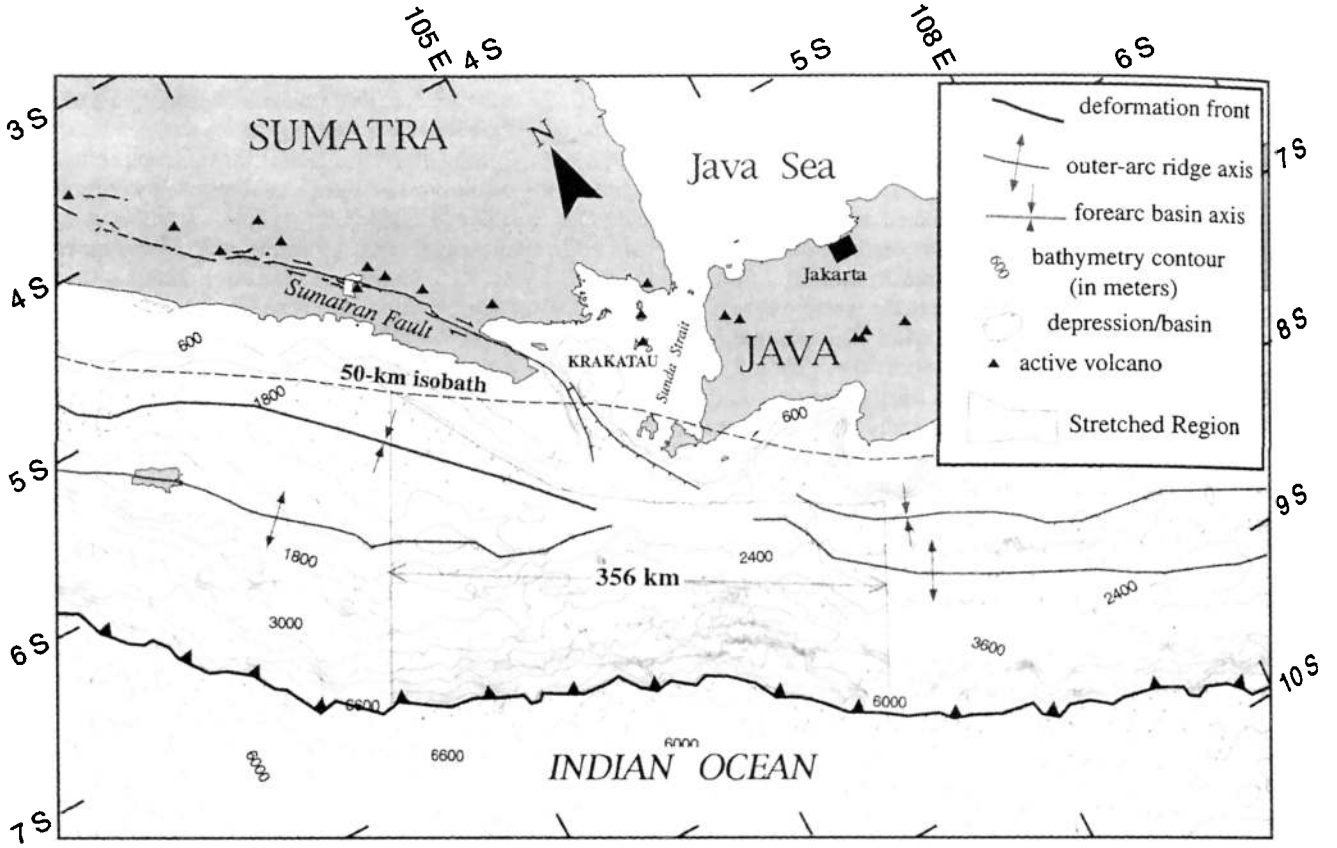

Figure 9. Stretching of the forearc sliver plate near the Sunda Strait, which appears to have thinned the forearc wedge perpendicular to the deformation front. By volumetric balancing, we calculate that ~100 km of stretching of the forearc sliver has occurred parallel to the Sumatran fault since formation of the outer-arc ridge and forearc basin. This would be a maximum value for northwestward translation of the part of the forearc sliver plate that is south of the equator.

Sumatran fault system has evolved significantly in the past several million years and that the current configuration of deformation is not representative of pre-Quaternary deformation.

One hundred kilometers of motion near the Sunda Strait contrasts markedly with the 460 km of opening suggested by *Curray et al.* [1979] for the Andaman spreading centers (Figure 1). The contrast disappears, if one compares Andaman extension and Sundan offset for similar periods of time. Only about 118 km of Andaman extension may have accumulated in the past 3 Myr (J. Curray, written communication, 1999). This does not differ greatly from the 100 km of stretching of the forearc near the Sunda Strait for about the same period of time (i.e. since the rapid rise of the Sumatran outer-arc ridge in the early Pliocene). Hence the discrepancy between deformation in the Andaman sea and Sunda Strait during the past 3 Myr may be very small or nonexistent.

Nonetheless, the current rate of slip on the Sumatran fault appears to diminish significantly from northwest to southeast. Although new geodetic evidence suggests that there is no significant decrease between about 1°S and 2°N [*Genrich et al.*, this issue], geologic slip rates across this section suggest a much larger decrease in rate, from 27 mm/yr (near 2.2°N) to 11 mm/yr (near 0.4°S) [*Sieh et al.*, 1991, 1994; D. Natawidjaja and K. Sieh, manuscript in preparation, 2000]. *Bellier and Sebrier's* [1995] estimations of slip rate along the fault, based upon correlations of stream length with age, also decrease from northwest to southeast.

If the total offset along the Sumatran fault is only ~20 km

Figure 10. (opposite) A plausible (but nonunique) history of deformation along the obliquely convergent Sumatran plate margin, based upon our work and consistent with GPS results and the timing of deformation in the forearc region. (a) By about 4 Ma, the outer-arc ridge has formed. The former deformation front and the Mentawai homocline provide a set of reference features for assessing later deformations. From 4 to 2 Ma, partitioning of oblique plate convergence occurs only north of the equator. Dextral-slip faults on the northeast flank of the forearc sliver plate parallel the trench in northern Sumatra but swing south and disarticulate the forearc basin and outer-arc ridge north of the equator. (b) Slip partitioning begins south of the equator about 2 Ma, with the creation of the Mentawai and Sumatran faults. Transtension continues in the forearc north of the equator. (c) In perhaps just the past 100 yr, the Mentawai fault has become inactive, and the rate of slip on the Sumatran fault north of 2°N has more than doubled. This difference in slip rate may be accommodated by a new zone of transtension between the Sumatran fault and the deformation front in the forearc and outer-arc regions.

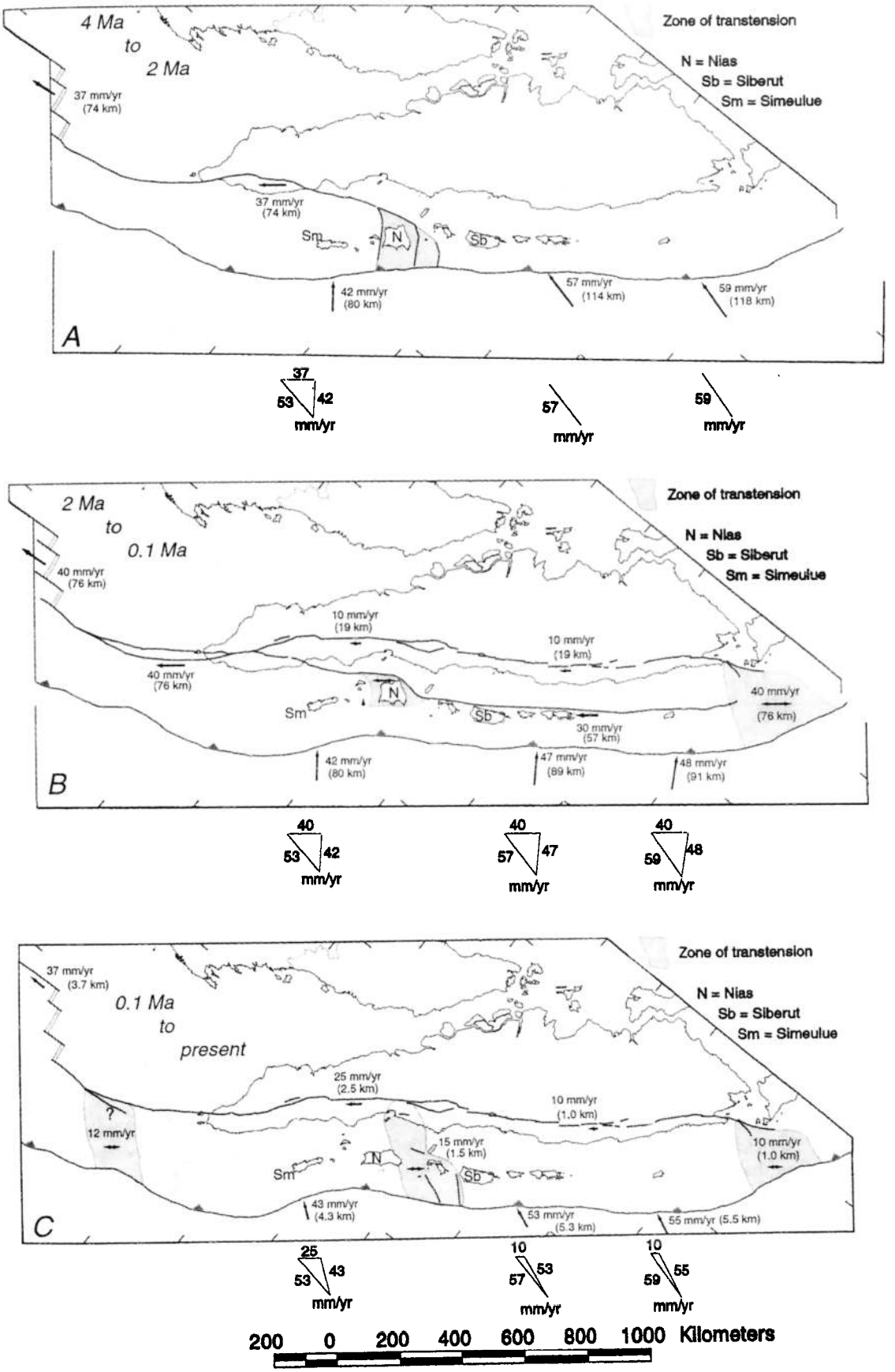
4 Ma
to
2 Ma
37 mm/yr
(74 km)
37 mm/yr
(74 km)
Sm
N
Sb
42 mm/yr
(80 km)
57 mm/yr
(114 km)
59 mm/yr
(118 km)
A
Zone of transtension
N = Nias
Sb = Siberut
Sm = Simeulue
37
53
42
mm/yr
57
mm/yr
59
mm/yr
2 Ma
to
0.1 Ma
40 mm/yr
(76 km)
10 mm/yr
(19 km)
10 mm/yr
(19 km)
40 mm/yr
(76 km)
Sm
N
Sb
30 mm/yr
(57 km)
40 mm/yr
(76 km)
42 mm/yr
(80 km)
47 mm/yr
(89 km)
48 mm/yr
(91 km)
B
Zone of transtension
N = Nias
Sb = Siberut
Sm = Simeulue
40
53
42
mm/yr
40
57
47
mm/yr
40
59
48
mm/yr
37 mm/yr
(3.7 km)
0.1 Ma
to
present
25 mm/yr
(2.5 km)
10 mm/yr
(1.0 km)
?
12 mm/yr
15 mm/yr
(1.5 km)
Sm
N
Sb
10 mm/yr
(1.0 km)
43 mm/yr
(4.3 km)
53 mm/yr
(5.3 km)
55 mm/yr (5.5 km)
C
Zone of transtension
N = Nias
Sb = Siberut
Sm = Simeulue
25
53
43
mm/yr
10
57
53
mm/yr
10
59
55
mm/yr
200 0 200 400 600 800 1000 Kilometers

and slip rates have been constant, then the northern part of the fault zone would be less than a million years old. South of the Equatorial Bifurcation, where late Quaternary slip rates appear to be ~10 mm/yr, 20 km of slip might have accrued in ~2 Myr.

Our calculation of ~100 km of fault-parallel stretching of the forearc near the Sunda Strait suggests that either the total offset along the Sumatran fault is much larger than 20 km or that another structure in the Sumatran fault system has accommodated ~80 km of the stretching. The only plausible other candidate for dextral slip would be the Mentawai fault, well constrained from seismic reflection data to run between the outer-arc ridge and the forearc basin [*Diament et al.*, 1992]. The linearity of the feature suggests that it is principally a strike-slip feature. *Diament et al.* [1992] also argue that the structure of the fault zone indicates that its sense is primarily strike-slip. In our opinion, the structural argument is a less compelling one because we are not convinced that the Mentawai fault zone exhibits the "flower" structure characteristic of strike-slip faulting. In fact, the position of the fault, on the northeastern flank of the outer-arc ridge, is consistent with the fault being a backthrust, along which the outer-arc ridge has risen. The existence of a large homocline in the same position relative to the forearc basin and outer-arc ridge north of the equator [*Karig et al.*, 1980] (Plate 1) supports this interpretation. So it is with some reluctance that, in the evolutionary model below, we use the Mentawai fault as a strike-slip element of the Sumatran fault system.

A final constraint on the evolution of the Sumatran fault system is the Mio-Pliocene history of the forearc and outer-arc regions. The Andaman spreading centers were actively spreading at ~40 mm/yr during this period, yet we have no evidence of contemporaneous dextral deformation of the forearc sliver plate south of the equator. How and where, in Pliocene and late Miocene time (about 2 to 10 Ma), was the dextral component of oblique convergence accommodated? *Matson and Moore* [1992] suggest that some of this discrepancy can be accommodated by the dextral-normal faults of the forearc region near Nias Island (Figure 2 and Plate 1). We consider this possibility below.

Stratigraphic and structural studies by *Samuel et al.* [1997] and *Samuel and Harbury* [1996] show that broadening and uplift of the outer-arc ridge occurred early in the Pliocene epoch throughout the Sumatran forearc region. This is critical to reconstructing deformation of the forearc sliver plate because the early Pliocene growth of the outer-arc ridge produced an elongate feature that has been deformed in the subsequent several million years. The ridge is clear in the bathymetry of Plate 1. South of about 1°S, it is regular and 60 to 80 km wide. Its northeastern boundary is the Pliocene Mentawai homoclinal flexure. On the southwest the ridge is bounded by a plateau that sits at a depth of ~2400 m. We speculate that this plateau was formerly a part of the Australian plate and that its northeastern edge is the former deformation front of the subduction zone. Similar features are also present between about 1.5°N and 3°N, near Simeulue Island.

Between 1.5°N and 2°S, the outer-arc ridge, the homocline, and the ancient deformation front and plateau are markedly disarticulated. *Karig et al.* [1980] observed that the Pliocene homocline on the east side of Nias is dextrally offset ~100 km by two strands of the Batee fault. We infer from bathymetry that the strand of the Batee fault northwest of Nias offsets the ancient deformation front ~50 km, from northwest of Nias to a position west of Nias (Plate 1). Farther south on the inner trench slope, between Nias and Siberut Islands, the deformation front may be offset by about an additional 50 km along another north striking fault.

Dextral offset of the eastern edge of the forearc basin by the Batee fault is ~150 km [*Karig et al.*, 1980]. From paleontologically constrained seismic stratigraphy, *Matson and Moore* [1992] show that the Batee fault was active from the late Miocene through the Pleistocene epochs. Twenty to thirty kilometers of dextral slip appear to have occurred on the nearby Singkel fault in the late Miocene epoch. Thus it is reasonable to suggest that the first few tens of kilometers of the 150-km dextral offset on the northern portions of the Batee fault accrued in the late Miocene. However, the bulk of the slip must be late Pliocene and younger because the Pliocene homocline of Nias Island is offset ~100 km. This offset must have accrued over at least 1.5 Myr, since a shorter duration would require rates of dextral slip in excess of the rate of relative plate motion.

Plate 1 also shows a disruption of the outer-arc ridge and inner trench slope south of Nias Island, at the Pini basin and between Tanabala and Siberut Islands. The Pini basin experienced rapid subsidence beginning about 4 Ma. This subsidence is probably contemporaneous with activity of north striking faults that bound the basin [*Matson and Moore*, 1992] and with minor north striking dextral-slip faults on Nias [*Samuel and Harbury*, 1996]. A disruption in the inner trench slope farther south, along strike of the Pini basin, may represent a 40- to 50-km dextral offset of the same ancient deformation front mentioned above.

Figures 10a-10c depict a plausible evolution of the Sumatran fault and other structures of the plate boundary that is consistent with available geologic, geodetic, and seismographic data. Variations of this history are also possible; our principal intention is to show that the fault system evolved significantly in the past few million years. The main characteristics of this speculative history are as follows: (1) the current 15 mm/yr difference in Sumatran fault slip rate north and south of the equator is very young (perhaps only100,000 years old), and (2) active normal- and dextral-slip (transtensional) faulting in the forearc and outer arc between 1°S and 2°N is an ancient (and perhaps current) analogue to the stretching at the southern end of the Sumatran fault.

Figure 10a shows the geometry of the region at about 4 Ma. Just prior to this time, relief between the forearc basin and the outer-arc ridge increased greatly across the homoclinal fold between the forearc basin and outer-arc ridge [*Karig et al.*, 1980; Samuel et al., 1997; *Samuel and Harbury*, 1996]. We speculate that as the outer-arc ridge grew, the subduction deformation front jumped southwestward to its present location, from a deformation front still visible in the bathymetry, closer to the outer-arc ridge (Plate 1). From 4 to 2 Ma, dextral slip on the Aceh segment and the Batee fault occurred at 37 mm/yr, and the homocline, outer-arc ridge, and inner trench slope were offset 37 km by a curved southern extension of the Batee fault, off the north coast of Nias Island, and 37 km more across the Pini basin. This is consistent with the stratigraphy of *Matson and Moore [1992]*. Several kilometers of arc-parallel elongation of Nias Island along north striking dextral-slip faults and conjugate sinistral-slip

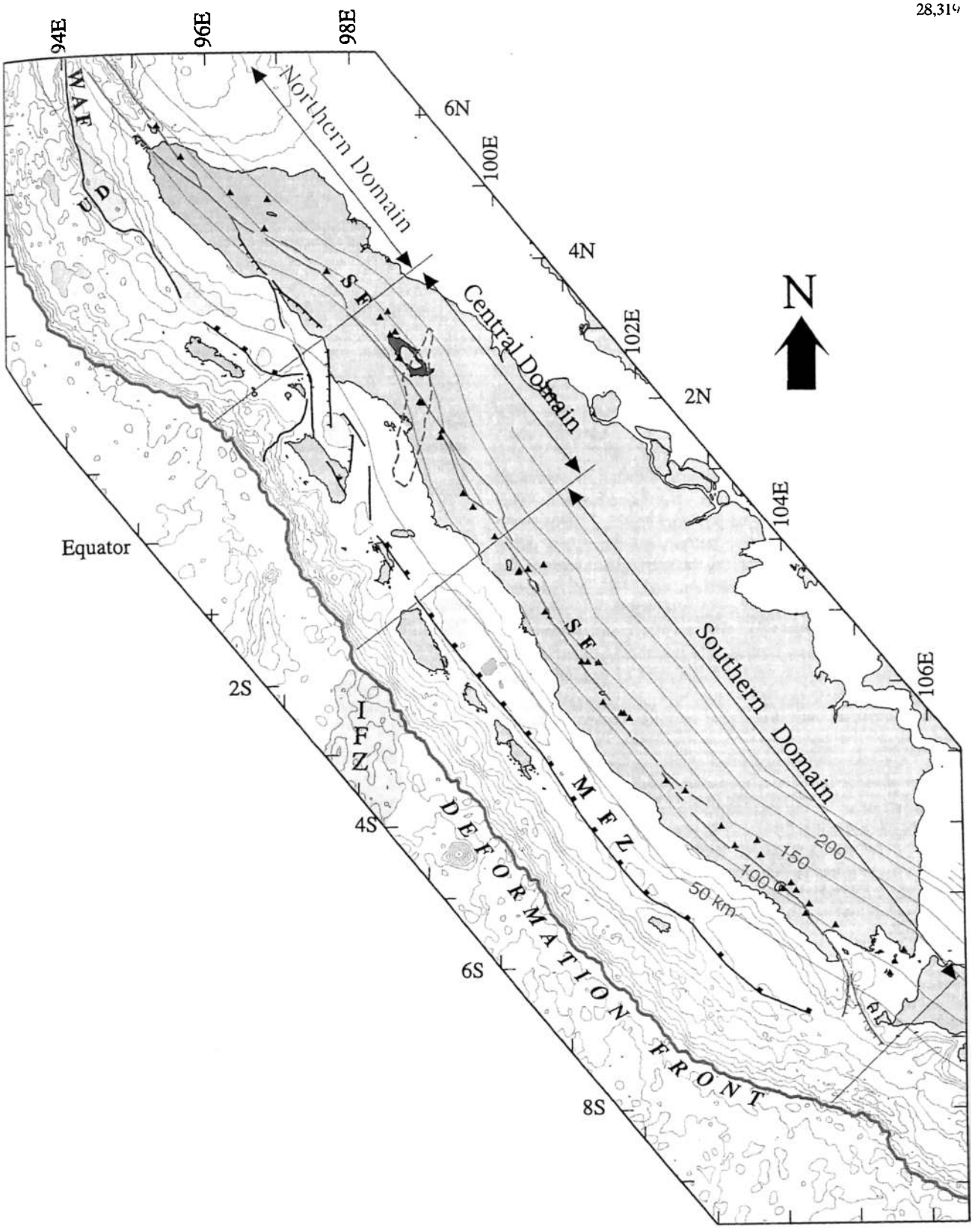

Plate 5. Geometric and structural details of the Sumatran fault, the forearc basin, outer-arc ridge, and volcanic arc, suggesting the division of the Sumatran plate margin into northern, central, and southern domains. The simplest outer arc, forearc, and Sumatran fault geometries are in the southern domain. The coincidence of this structural domain with the source region of the giant (M_w 9) subduction earthquake of 1833 suggests that geometrical simplicity encourages large ruptures. The central domain appears to have been the source region of the great (M_w 8.4) subduction earthquake of 1861. Fragmentation of the central domain appears to have been caused by subduction of the Investigator fracture zone during the past 5 Myr. The locus of impingement of the fracture zone on the deformation front was calculated by assuming the current relative plate motion vector and the forearc deformation history of Figure 10. Contours in red are the top of the Benioff-Wadati zone. Bathymetric contour interval is 200 m.

faults also occurred during this period [*Samuel and Harbury*, 1996]. Subduction south of the equator was parallel to the relative plate motion vector and highly oblique to the deformation front. Subduction north of the equator was mostly or wholly dip slip because most or all of the dextral component of plate motion was occurring along the Batee-Aceh fault.

About 2 Ma (Figure 10b), both the Mentawai fault and the Sumatran fault formed. From 2 Ma to 100 ka, they carried ~40 mm/yr of the dextral component of oblique convergence south of the equator, and the subduction interface accommodated only the dip-slip component. North of the equator, 40 mm/yr of dextral slip was accommodated by the Sumatran fault (10 mm/yr) and Aceh-Batee fault (30 mm/yr).

Figure 10c depicts our suggestion for the current neotectonic partitioning of deformation. The Aceh-Batee fault is no longer active or is only minimally so. The Sumatran fault is slipping ~15 mm/yr faster north of about 2°N than south. The mass balance problem caused by this discrepancy is being taken up by a nascent belt of deformation that crosses the outer-arc ridge at the equator. This deformation belt is superjacent to *Fauzi et al.'s* [1996] swath of exceptionally high seismic activity in the down going oceanic slab. It also encompasses the active Toru folds of the mainland coast, two young faults on and south of Nias and north-south graben that bathymetry suggest may exist on the inner trench slope (Plate 1). Figure 10c is consistent with recent measurements of geologically measured Sumatran fault slip rates but is inconsistent with the rates of geodetic strain measured by GPS south of the equator.

If the Sumatran fault is carrying only ~10 mm/yr of dextral slip south of the equator [*Sieh et al.*, 1994; *Bellier et al.*, 1999], the remainder of the dextral component of slip must be taken up along either the subduction interface or by a fault within the forearc sliver. The GPS data show no sharp gradients in shear in the forearc region, so the remaining dextral component is probably accommodated by slip on the subduction interface [*McCaffrey et al.*, this issue]. This portion of the dextral component, x, would be ~27 mm/yr (x = 58 mm/yr*sin 41° - 10 mm/yr, where 58 mm/yr is the magnitude of relative plate motion and 41° is the angle between the plate motion vector and the trench normal and 10 mm/yr is the slip rate on the Sumatran fault). Slip vectors for earthquakes on the subduction interface deviate from the trench normal by ~20°, on average. These suggest that the dextral component on the interface would be a bit less than our model predicts, only ~16 mm/yr.

The history depicted in Figure 10 is consistent with the timing of activity on faults both offshore and onshore Nias [*Karig et al.*, 1980; *Matson and Moore*, 1992; *Samuel and Harbury*, 1996]. It also incorporates our observation that the Batee fault is not currently active along most of its exposed trace but retains clear evidence of 5-km dextral offsets of a few of the largest channels that cross it (Plate 1). Restoration of ~80 km of slip on the faults between 1°S and 2°N in the offshore region eliminates the dimple in the subduction deformation front west of Nias and Simeulue, just as restoration of ~80 km of slip on the combined Sumatran and Mentawai faults nearly eliminates the dimple west of the Sunda Strait. Thus we suggest that the concavities of the deformation front west of Nias and west of the Sunda Strait are features inherited from Plio-Pleistocene dextral strike-slip motion in the forearc region.

3.3. Tectonic Model of the Sumatran Plate Margin

Transtensional necking of the forearc region between 1°S and 2°N during the past 4 Myr has had a profound effect on all of the major elements of the plate margin there. The inner trench slope, outer-arc ridge, and forearc basin have been fragmented by this process. Even the shapes of the subduction interface, the active volcanic arc, and the Sumatran fault appear to have been affected. In fact, we can divide the Sumatran plate boundary into three tectonic domains, based upon their relationship to this Plio-Pleistocene transtension (Plate 5). The southern domain, which we suggest has been part of the forearc sliver plate only for the past 2 Myr, is the most simple geometrically and structurally. The central domain, which comprises all the transtensionally fragmented pieces, is the most complex.

The southern domain has the following characteristics: (1) the Sumatran fault displays a right-stepping en echelon pattern and courses above the 100- to 135-km isobaths of the subduction interface, (2) the locus of volcanism is predominantly northeast of or near the fault, (3) the forearc basin is remarkably simple, ~2 km deep and unbroken by major faults, (4) the outer-arc ridge is relatively narrow, forms a single antiformal high, and is geometrically simple, (5) the Mentawai fault and homocline, which separate the basin and ridge, are unbroken and relatively straight, and (6) the inner trench slope is relatively uniform and possesses a prominent plateau about half way between the active deformation front and the outer-arc ridge. The source of the giant (M_w 9) subduction earthquake of 1833 was the subduction interface beneath much of this domain [*Newcomb and McCann*, 1987; *Zachariasen et al.*, 1999]. Strains measured by GPS in the early to mid-1990s show that the outer-arc islands are moving parallel to the relative plate motion vector and that the subduction interface beneath the southern domain is currently fully locked [*Prawirodirdjo et al.*, 1997; *McCaffrey et al.*, this issue]. The Sumatran fault appears to be slipping at a rate of about 10 mm/yr in the Southern domain [*Sieh et al.*, 1991, 1994; *Bellier et al.*, 1999].

The northern domain is characterized by these features: (1) a geometrically irregular Sumatran fault, with both releasing and restraining bends, which resides above the 125- to 140-km subduction isobaths, (2) a volcanic arc on and north of the Sumatran fault, (3) a 1- to 2-km-deep forearc basin, (4) a very broad, structurally and bathymetrically complex outer-arc ridge, (5) a homocline along its southernmost few hundred kilometers that is similar to the Mentawai structure of the southern domain, and (6) a very narrow inner trench slope.
The central domain is distinguished by these features: (1) a 350-km-long section of the Sumatran fault that is markedly discordant with the subduction isobaths, (2) a volcanic arc that cuts dramatically across the Sumatran fault, (3) a topographically shallow (0.2-0.6 km deep) forearc basin, which has been fragmented into several blocks during oblique-normal faulting, (4) a fragmented outer arc, (5) a fragmented homocline between the outer-arc ridge and forearc basin, and (6) a fragmented inner trench slope. The giant (M_w 8.5) subduction earthquake of 1861 and numerous other large historic subduction earthquakes originated within this domain [*Newcomb and McCann*, 1987]. Strains measured by GPS in the early to mid-1990s indicate that the hanging wall block across the central domain is currently moving parallel to the subduction deformation front [*Prawirodirdjo et al.*, 1997;

McCaffrey et al., this issue]. The geologic rate of slip of the Sumatran fault increases markedly from southeast to northwest across the central domain, from ~11 mm/yr to ~27 mm/yr [*Sieh et al.*, 1991].

We suspect that transtensional fragmentation has dominated the central domain because the Investigator fracture zone has been subducting beneath the central domain for the past several million years. Its locus of impingement on the deformation front has migrated from the northern to the southern margin of the central domain during the past 5 Myr (Plate 5). This may be significant because fault activity in the hanging wall block of the forearc region appears to have been restricted during this period to the central domain (Figure 10). Furthermore, the orientations of faults in the central domain are predominantly north-south, parallel to the topographic and structural grain of the underlying Investigator fracture zone. We hypothesize therefore that the topographic heterogeneity of the Investigator fracture zone beneath the central domain has led to disruption of the forearc and outer-arc regions. Currently, the Investigator fracture zone is also associated with a band of intense seismicity within the down going slab in the middle of the central domain (Plate 5) [*Fauzi et al.*, 1996] and an abrupt change in the azimuth of GPS vectors on the outer-arc ridge [*Prawirodirdjo et al.*, 1997, *McCaffrey et al.*, this issue].

The subduction interface curves broadly across the Central domain (Plate 5) [*Fauzi et al.*, 1996]. The close association of this curve with the other elements of the central domain suggests cause and effect or at least a shared cause. Could flexure of the downgoing slab have been produced by necking of the hanging wall block? Or did deformation within the downgoing slab lead to transtension in the forearc sliver plate? We suggest the former.

The existence of the 1500-km-wide boundary between Indian and Australian plates offshore western Sumatra and the Andaman Islands gives reason to suspect that the downgoing slab west of the Investigator fracture zone is deforming. This broad region of deformation abuts all of the central and northern domains. *Gordon et al.* [1990] calculate that the two oceanic plates are converging north-south at an angular rate of 0.3°/Myr about a pole of rotation in the central Indian Ocean. At the Sumatran deformation front this translates into a nominal 13-km north-south shortening of the downgoing slab in the past 3 Myr. The actual nature of lithospheric deformation west of the deformation front is quite uncertain, however. Simple north-south buckling is unlikely. Focal mechanisms and structure indicate a predominance of north-south left-lateral slip on north-south faults [*Deplus et al.*, 1998]. To accommodate north-south contraction, these structures would need to be rotating clockwise, domino-like, to enable eastward extrusion of lithosphere [*Gordon et al.*, 1990]. The precise loci of such deformation is unknown, and so its impact on the overriding central and northern domains is hard to assess. Nonetheless, it is plausible that the contrast in nature of the southern and northern hanging wall domains could have arisen, at least in part, from subduction of deforming oceanic lithosphere beneath the northern domain. It is hard to imagine, however, how dextral transtension on north striking faults within the central domain could be related to sinistral slip and clockwise rotation on north striking faults in the subjacent subducting lithosphere, unless eastward extrusion of the oceanic lithosphere has led to northwestward extrusion of the forearc sliver plate, as plate collision has done in Turkey and Tibet.

A more logical proposition may be that transtensional necking of the central domain has led to bending of the subducting slab Trench-orthogonal thinning of the forearc appears to have drawn the deformation front and trench northeastward, tens of kilometers closer to the mainland coast. If this process had not also drawn the deeper parts of the subducting slab northeastward, the dip of the interface in the forearc and outer arc would be steeper than in the southern domain. The isobaths show the contrary, that the subduction zone beneath the central domain has a very similar cross-sectional profile to that beneath the southern domain. One test of this hypothesis would be to determine if the active volcanic arc in the central domain is substantially northeast of the late Miocene and Pliocene arc. If so, it would suggest that the subduction isobaths have moved northeastward in the past few million years.

3.4. Relationship of the Sumatran Fault to the Modern Volcanic Arc

Many have noted the proximity of the Sumatran fault to the volcanic arc and have suggested that it formed there because of the effect of magmatism on the lithosphere [e.g., *Fauzi et al.*, 1996; *Tikoff*, 1998]. Sumatra aside for the moment, however, most trench-parallel strike-slip faults are not coincident with their volcanic arcs. The Median Tectonic Line (Japan) does not have an associated arc; the Denali fault (Alaska) lies much farther from the trench than the Alaskan arc volcanoes; the Atacama fault (Chile) lies between the trench and volcanic arc; and the Philippine fault is tens of kilometers from the major Philippine arc volcanoes [*Yeats et al.*, 1997]. Furthermore, most volcanic arcs along obliquely convergent margins do not sport large strike-slip faults. This general lack of association suggests that the alignment of the Sumatran volcanic arc and the Sumatran fault is purely a coincidence. In fact, *McCaffrey et al.* [this issue] have used finite element modeling of stresses across the obliquely convergent Sumatran plate boundary to show that formation of the trench-parallel Sumatran fault did not require the presence of the magmatic arc. Nonetheless, *Tikoff* [1998] has suggested that faults such as the Sumatran fault form above the locus of greatest strain gradient in the lower crust or mantle, occasioned by the magmatism of the volcanic arc. *Bellier and Sebrier* [1994] have claimed that numerous small and large volcanic cones and calderas occur at both current and ancient releasing step overs along the Sumatran fault.

We can test directly whether or not magmatism has influenced the location of the fault or, conversely, whether or not faulting has influenced the location of volcanism and magmatism. Plate 1 allows us to search for a relationship between the volcanic arc and the Sumatran fault, since it displays not only the most prominent traces of the Sumatran fault but also the youngest volcanoes. We mapped these volcanic features using the same sources we used to map the fault (Figure 2). We limited our mapping to those features that have suffered minimal erosion, since highly eroded, older volcanic constructs are harder to recognize geomorphologically and mapping would have required a more substantial effort. The features we mapped exhibit very little erosional modification of their constructional landforms. Many have been active historically. Those that have been dated radiometrically are typically <100,000 years old (e.g., Toba caldera, 73 ka [*Chesner et al.*, 1991], and Maninjou caldera, 60-90 ka [*Nishimura*, 1980]). In addition to mapping

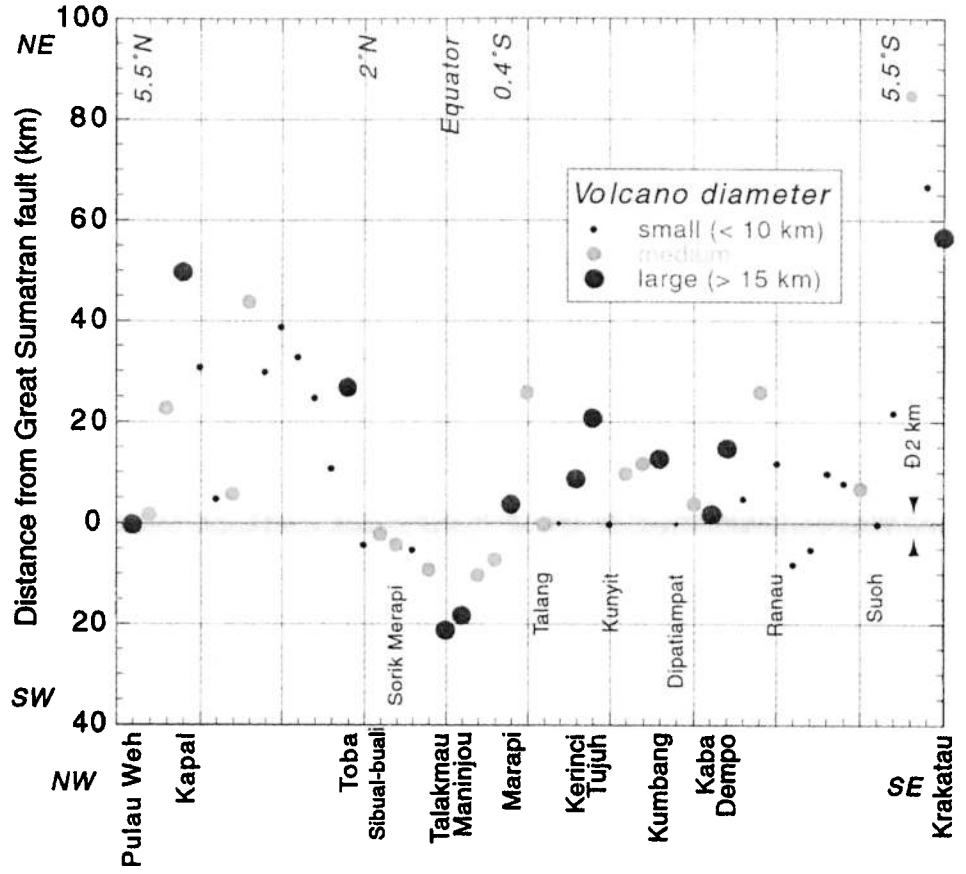

Figure 11. Plot of the distance of volcanic centers from the Sumatran fault showing that the volcanic arc has not influenced the location of the fault. However, 9 of the 50 volcanic centers are within 2 km of the fault. Most of these are associated with extensional (right) step overs in the fault. Large (15-km diameter) volcanic edifices are listed along the horizontal axis. Smaller volcanoes mentioned in the text are named.

craters and calderas, which are indicators of volcanic source vents, we also mapped the edges of the volcanic cones in order to display a crude measure of the output of individual sources.

At first glance, the most striking relationships between the Sumatran fault and the young arc volcanoes are that: (1) the average center line of the active arc is decidedly landward (northeast) of the Sumatran fault and (2) the local center line of the young volcanic arc switches back and forth across the trace of the Sumatran fault as it traverses the 1650-km length of Sumatra. Figure 11 shows these relationships. The 10-km separations northeast from the Sumatran fault are common, 25-km distances are not rare, and a few volcanoes are even farther northeast. Only two volcanoes are more than 10 km southwest of the Sumatran fault. From Figure 11 one can estimate that the averaged center line of the largest volcanic edifices is ~10 km northeast of the Sumatran fault. This skewed distribution of volcanoes relative to the Sumatran fault suggests that the modern magmatic arc has not created a weak crustal zone that has favored the concentration of shear. Perhaps the active volcanic arc has failed to influence the locus of faulting because the volcanic conduits "soften" only a small percentage of the length of the arc. Alternatively, perhaps magmatic plumbing beneath the Sumatran fault, associated with an unmapped, extinct volcanic arc, did influence the location of the fault.

The local center line of the volcanic arc varies along the strike of the Sumatran fault. It is a few kilometers northeast of the fault between 5.5°S and 0.4°S, swings southwest of the Sumatran fault between 0.4°S and about 2°N, and then swings to a position ~25 km northeast of the Sumatran fault between 2°N and 5.5°N. This broad disparity between the local center line of the volcanic arc and the Sumatran fault is another indication that modern arc magmatism has not guided the formation of the fault.

It also does not appear that individual volcanic conduits have influenced the location of particular fault segments. Only rarely do individual segments of the fault bisect volcanic centers or bend in their vicinity (counterexamples are Kaba and Dipatiampat). However, we would not expect such an association, since the volcanoes that we have mapped are far younger than the age of initiation of the mapped fault segments. We suspect that most of the uneroded edifices are less than 100,000 years old, whereas we have made a case that the fault planes we have mapped are probably ~2 Myr old. If the locus of faulting were influenced by magmatic softening of the crust, the magmatic plumbing that led to the concentration of strains beneath the Sumatran fault would have formed long before the young volcanoes on Plate 1. To test the hypothesis that magmatic concentration of shear stresses led to the formation of the fault within the arc, one would need to map the Pliocene and early Pleistocene

volcanic centers. We may attempt this at a future date, but it is beyond the scope of our current efforts.

Despite the lack of influence of active magmatism on tectonism, tectonism is influencing magmatism, but only to a minor extent. This conclusion contrasts with that of *Bellier and Sebrier* [1994], who proposed that extensional pull aparts along the Sumatran fault have affected the location of the volcanoes. In fact, our map shows that only 9 of the 50 young volcanic vents shown on Plate 1 are located within 2 km of a mapped trace of the Sumatran fault (Figure 11). These are, from southeast to northwest, Suoh, Seminung, Kaba, Dipatiampat, Kunyit, Melenggok, Talang, Sibual-buali, Seulawah Agam, and Pulau Weh. Kaba, Kunvit, Meleggok, Talang, Sibual-buali, Seulawah Agam, and Pulau Web are stratovolcanoes greater than about 10 km in diameter and, thus, embody the most substantial volumes. Suoh, Kaba, Kunyit, Melenggok, Talang, and Sibual-buali are located within dilatational stepovers or on one of the bounding faults of a dilatational step over. One of these (Suoh) is a large phreatic explosion crater that formed 15 days after the large Semangko segment rupture of 1933 [*Stehn*, 1934], most convincingly in association with tectonic activity. *Bellier and Sebrier* [1994] proposed that Toba and Ranau calderas also formed at extinct extensional step overs along the Sumatran fault zone, but these hypotheses are not well founded. They are based solely on the use of SPOT imagery to map more ancient fault strands in the vicinity of these two calderas. Although lineations may exist along these alleged ancient faults, their documentation of the lineations is scant, and they present no geologic mapping to confirm their existence or to quantify the style, age, or amount of shear along them.

We suspect that the association of just 9 of the 50 young volcanoes with the Sumatran fault is a random occurrence. If one peppered an elongate rectangle (with the 1700-by-50 km dimensions of the volcanic arc) with a random distribution of 50 points and then ran straight lines randomly through its long dimension, several points would typically be within 2 km of each line. Thus the close association of several volcanoes with the Sumatran fault zone does not, by itself, demonstrate a genetic relationship. The close association of six of the eight close encounters with dilatational step overs does, however, suggest that tectonic step overs are influencing the locations of a few of the arc's volcanic centers.

3.5. Relationship of the Sumatran Fault to the Subduction Zone

The general shape of the Sumatran fault mimics that of the deformation front offshore so faithfully that one wonders about a genetic relationship between the subduction interface and the strike-slip fault (Plate 5). North of the equator, both structures are concave toward the southwest. South of the equator, both are broadly concave toward the northeast. Along the entire length of the Sumatran fault on land, its horizontal distance from the deformation front varies no more than ~10% from 290 km (Table 1 and Plate 5).

A similar coincidence exists between the shape of the Sumatran fault and that of the subduction interface downdip from its trace. This is clear from Plates 1 and 5, which show the 50-, 100-, and 200-km isobaths of the subduction interface. The contours are drawn on the top of the Wadati-Benioff zone, as defined by hypocentral locations in the International Seismological Center (ISC) catalog (as relocated by *Engdahl et al.* [1998]) and as determined by *Fauzi et al.* [1996] in their local seismic survey in the region of Lake Toba.

From about 6°S to the equator, the relationship is particularly regular; the subduction interface lies 100 to 135 km below the Sumatran fault, except along the southernmost (Sunda) segment (Plate 1 and Table 1). Between about 3.5°N and 6.0°N the subduction interface is 125 to 140 km below the Sumatran fault, except beneath the northern (possibly inactive) part of the Aceh segment. These depths in the north are, on average, ~20 km greater than depths south of the equator. The relationship of subduction isobaths to the Sumatran fault is markedly aberrant between the equator and about 3.5°N. There the traces of the Sumatran fault and the subduction isobaths are markedly discordant; the depth of the interface beneath the Sumatran fault ranges from ~100 to 175 km.

Because of the well-behaved relationship of Sumatran fault to isobaths in the northern and southern domains, we propose that the Sumatran fault formed first in those two domains, as two separate structures. As displacement on the faults has grown, they have formed a linkage across the central domain and will one day become a single structure.

4. Summary, Conclusions, and Remaining Questions

We have used stereographic aerial photography and topography to map 1650 km of the Sumatran fault (Figures 2 and 3). The resulting map shows that the fault comprises numerous segments separated by dilatational and contractional step overs and abrupt changes in trend (Plate 1 and Figure 4). This segmentation appears to have influenced the rupture dimensions of historical large earthquakes and limited their magnitudes to ~7.5.

The largest geomorphically evident offsets along the Sumatran fault are between 17 and 23 km (Plate 3, Figures 7, and 9 and Table 3). These are predominantly deeply incised river channels, but one apparent offset of a fold pair and the accumulated offset across a major step over also fall within this range. A lack of detailed and complete mapping along the fault precludes confident matching of geologic units across the fault, but rock offsets suggested by *Katili and Hehuwat* [1967] and *Cameron et al.* [1983] support the contention that the 20-km geomorphic offsets represent the total offset across the fault.

The distention of forearc structures and the trench near the Sunda Strait suggests ~100 km of arc-parallel stretching of the forearc sliver plate since the early Pliocene (Figures 5 and 8). We propose that 20 km of this was accommodated by dextral slip on the Sumatran fault and that the Mentawai fault, a long, linear structure within the forearc region, accommodated the remaining dextral slip.

Our synthesis of data from the Sumatran fault, the volcanic arc, and the forearc region shows that the Sumatran forearc sliver plate consists of three tectonic domains with very distinct tectonic histories (Plate 5). The southern domain (from 7°S to 1°S) is the simplest and may have been accreted to the forearc sliver plate only about 2 Myr ago by the creation of the Sumatran and Mentawai faults. The northern domain (north of 2°N) is more complex, and its northern part has been experiencing arc-parallel translation for at least the

past 10 Myr. The central domain is the most complex of the three and has been a region of transtension between the northern and southern domains since at least 4 Myr ago.

Geodetic measurements suggest that slip across the Sumatran fault between about 0.8° S and 2.7°N is nearly uniform at about 25 mm/yr [*Genrich et al.*, this issue]. These rates are incompatible with the 27 and11 mm/yr geologic slip rates that we have determined at 2.2°N and 0.3°S [*Sieh et al.*, 1991, 1994; D. Natawidjaja and K. Sieh, manuscript in preparation, 2000). We propose that the geologic difference in rates has arisen in just the past 100 ka or so, because structural evidence for accommodation of the 15 mm/yr difference is obscure. We suggest that a belt of auxiliary, transtensional deformation between the Sumatran fault and the trench is the nascent manifestation of this rate change (Figure 10). This belt includes the western (Angkola) branch of the Equatorial Bifurcation, the Toru fold-and-thrust belt along the mainland coast, and submarine faults in the forearc basin, outer-arc ridge, and inner trench slope.

Although the Sumatran fault and the Sumatran volcanic arc share the same jungle, neither appears to have fundamentally affected the location of the other. Rather than being coincident, the fault and the arc intertwine (Figure 11). The averaged center line of the volcanic arc is distinctly northeast of, not at, the Sumatran fault. Nevertheless, the few volcanic centers that are on or very near the Sumatran fault are predominantly at major extensional step overs, which may well have attracted a small percent of the arc volcanism. The dramatic bend in the modern volcanic arc between 0.7°N and 2.5°N is most probably the result of transtensional thinning of the forearc sliver plate in the past 4 Myr. We can not rule out the possiblility that the Pliocene and Miocene volcanic arc were less sinuous and closer to the locus of later strike-slip faulting.

The broad similarity in shape of the Sumatran fault and subduction interface suggests a genetic relationship. The broad, low-amplitude sinusoidal shape of the subduction interface is mimicked by the Sumatran fault, and along most of its trace the Sumatran fault lies above the 110- to 140-km isobaths of the subduction interface. These relationships are particularly regular north of 3.5°N and south of the equator, in the northern and southern domains. We suggest that the Sumatran fault first formed as two separate faults in these two domains, and are in the process of linking together through the central domain and across the volcanic arc. We ascribe the disrupted nature of the central domain's outer-arc ridge and forearc basins to its location above the Investigator fracture zone throughout the past 5 Myr.

Not unexpectedly, this work has generated as many questions as answers: What are the details of the creation and evolution of the three tectonic domains of the forearc sliver plate? How, for example, did deformation in the transtensional central domain evolve through the past several million years? Why did the Sumatran fault form where it did, 290 km from the subduction deformation front and 100 to 150 km above the subduction interface? Would careful, detailed mapping confirm total Sumatran fault offsets of only ~20 km? When did the contrast in slip rates along the Sumatran fault begin? Why is this gradient in rates not apparent in the geodetic data? Is it plausible that the Mentawai fault has a strike-slip component as large as 80 km? Did the two faults originate a mere 2 Myr ago?

Our map of the Sumatran fault can serve as a jumping-off point for careful analysis of the seismic hazard posed by this major structure. To what degree does the historical record of large earthquakes along the Sumatran fault demonstrate that large structural irregularities constrain rupture lengths? Would primitive instrumental records help constrain the source parameters of these large events of the first half of the twentieth century? Whether or not segmentation of the Sumatran fault has markedly influenced ruptures, answering these questions could profoundly affect our general understanding of the importance of structural geometry on seismic rupture processes.

Acknowledgments. This work began with an invitation by Yehuda Bock and his colleagues at the Indonesian National Coordination Agency for Surveying and Mapping (BAKOSURTANAL) to visit Sumatra. They were interested in establishing a better geologic context for their GPS geodetic studies, supported under NSF grants EAR-8817067 and EAR-9004376. Our initial reconnaissance, in 1991, supported by donations from the Caltech Associates, convinced us that geological work aimed at understanding the active tectonics of the fault could be very fruitful. In 1992, we initiated our own NSF sponsored project (EAR-9205591) to map and characterize the Sumatran fault. BAKOSURTANAL, through Bock, supplied most of our topographic coverage of the fault. We are grateful to Suparka and Hery Harjono at the Indonesian Institute of Sciences (LIPI) for helping us acquire many important aerial photographs and arranging fieldwork. Rudy Bachruddin at the Volcanological Survey of Indonesia (VSI) and Gunawan Burhan at the Geological Research and Development Centers (GRDC) also helped us by providing essential aerial photographs along portions of the Sumatran fault. Various private companies also allowed us access to topographic maps and aerial photographs. Paul Tapponnier (IPG Paris) shared topographic maps from the Singkarak region. We also benefited from conversations with Rob McCaffrey and Bob Kieckhefer and from an initial GIS compilation of our data by Carolyn White. Reviews of an early manuscript by Yehuda Bock, Joseph Curray, and Rob McCaffrey were very helpful. Finally, we greatly appreciate the thorough, thoughtful, and careful reviews of Jeff Freymuller, Eli Silver, and Paul Tapponnier. This is Caltech Seismological Laboratory contribution 8625.

References

Abe, K., Magnitudes of large shallow earthquakes from 1904 to 1980: *Phys. Earth Planet. Inter. 27*, 72-92, 1981.

Allen, C., A. Gillespie, H. Yuan, K. Sieh, Z. Buchun, and Z. Chengnan, Red River and associated faults, Yunnan Province, China: Quaternary geology, slip rate and seismic hazard, *Geol. Soc. Am. Bull.*, 95, 686-700, 1984.

Allen, C.R., San Andreas fault zone in San Gorgonio Pass, southern California, *Geol. Soc. Am. Bull.*, 68, 315-350, 1957.

Armijo, R., B. Meyer, and A. Hubert, Westward propagation of the North Anatolian fault into the northern Aegean: Timing and kinematics, *Geology, 27*, 267-270, 1999.

Aspden, J.A., W. Kartawa, D.T. Aldiss, A. Djunuddin, R. Whandoyo, D. Diatma, M.C.G. Clarke, and H. Harahap, The geology of the Padangsidempuan and Sibolga Quadrangle, Sumatra, report Geol. Res. and Dev. Centr., Bandung, Indonesia, 1982.

Barka, A., The North Anatolian fault zone, *Ann. Tectonicae, 6*, 164-195, 1992.

Bellier, O., and M. Sebrier, Relationship between tectonism and volcanism along the Great Sumatran fault zone deduced by SPOT image analyses, *Tectonophysics, 233*, 215-231, 1994.

Bellier, O., and M. Sebrier, Is the slip rate variation on the Great Sumatran fault accommodated by fore-arc stretching?: *Geophys. Res. Lett.*, 22 1969-1972, 1995.

Bellier, O., M. Sebrier, S. Pramumidjojo, T. Beaudouin, H. Harjono, I. Bahar, and O. Forni, Paleoseismicity and seismic hazard along the Great Sumatran fault (Indonesia), *J. Geodyn., 24*, 169-183, 1997.

Bellier, O., H. Bellon, M. Sebrier, Sutanto, and R. Maury, K-Ar age of the Ranau Tuffs: Implications for the Ranau caldera emplacement and slip-partitioning in Sumatra (Indonesia), *Tectonophysics, 312*, 347-359, 1999.

Bennett, J. D., et al., Geologic map of the Banda Aceh quadrangle, Sumatra, Geol. Res. and Dev. Cent., Bandung, Indonesia, 1981.

Berlage, H., Jr., De aardbeving in zuid Sumatra van 25 Juni 1933: Waarremingen in het epicentrale gebied, *Natuurwet. Tijdschr. Ned. Indie, 94*, 15-36,1934.

Cameron, N., M. Clarke, D. Aldiss, J. Aspden, and A. Djunuddin, The geological evolution of northern Sumatra, paper presented at Proc. 9th Indonesian Petroleum Association Annual Convention, Jakarta, 1980.

Cameron, N., et al., Geology of the Takengon quadrangle, Sumatra, report Geol. Res. and Dev. Cent., Bandung, Indonesia, 1983.

Chesner, C.A., W. I. Rose, A. Deino, R. Drake, and J. A. Westgate, Eruptive history of Earth's largest Quaternary caldera (Toba, Indonesia) clarified, *Geology, 19*, 200-203, 1991.

Curray, J., D. Moore, L. Lawver, F. Emmel, R. Raitt, M. Henry, and R. Kieckhefer, Tectonics of the Andaman Sea and Burma, *AAPG Mem., 29*, 189-198, 1979.

Deplus, C., et al., Direct evidence of active deformation in the eastern Indian oceanic plate, *Geology, 26*, 131-134, 1998.

Detourbet, C., O. Bellier, and M. Sebrier, La caldera volcanique de Toba et le systeme de faille de Sumatra (Indonesia) vue par SPOT, *C. R. Acad. Sci., Ser. II, 316*, 1439-1445, 1993.

Diament, M., H. Harjono, K. Karta, C. Deplus, D. Dahrin, M. T. Zen Jr., M. Gerard, O. Lassal, A. Martin, and J. Malod, Mentawai fault zone off Sumatra: A new key to the geodynamics of western Indonesia, *Geology, 20*, 259-262, 1992.

Durham, J., Oeloe Aer fault zone, Sumatra, *Bull. Am. Assoc. Pet Geol., 24*, 359-362, 1940.

Engdahl, E., R. van der Hilst, and R. Buland, Global teleseismic earthquake relocation with improved travel times and procedures for depth determination: *Seismol. Soc. Am. Bull. 88*, 722-743, 1998.

Fauzi, R. McCaffrey, D. Wark, Sunaryo, and P. Y-PrihHaryadi, Lateral variation in slab orientation beneath Toba caldera, northern Sumatra, *Geophys. Res. Lett., 23*, 443-446, 1996.

Fitch, T. J., Plate convergence, transcurrent faults, and internal deformation adjacent to southeast Asia and the western Pacific, *J. Geophys. Res., 77*, 4432-4462, 1972.

Genrich, J., Y. Bock, R. McCaffrey, L. Prawirodirdjo, C. Stevens, S. S. O.Puntodewo, C. Subarya and S. Wdowinski, Distribution of slip at the northern Sumatra fault system, *J. Geophys. Res.*, this issue.

Gordon, R., C. Demets, and D. Argus, Kinematic constraints on distributed lithospheric deformation in the equatorial Indian ocean from present motion between the Australian and Indian plates: *Tectonics 9*, 409-422, 1990.

Harbury, N., and H. Kalagher, The sunda outer-arc ridge, north Sumatra, Indonesia, *J. Southeast Asian Earth Sci., 6*(3/4), 463-476, 1991.

Harjono, H., M. Diament, J. Dubois, and M. Larue, Seismicity of the Sunda Strait: Evidence for crustal extension and volcanological implicationa, *Tectonics, 10*, 17-30, 1991.

Harris, R., and S. Day, Dynamics of fault interaction: Parallel strike-slip faults, *J. Geophys. Res., 98*, 4461-4472, 1993.

Harris, R., R. Archuleta, and S. Day, Fault steps and the dynamic rupture process: 2-D numerical simulations of a spontaneously propagating shear fracture, *Geophys. Res. Lett., 18*, 893-896, 1991.

Huchon, P., and X. Le Pichon, Sunda Strait and central Sumatra fault, *Geology, 12*, 668-672, 1984.

Jarrard, R., Terrane motion by strike-slip faulting of fore-arc slivers, *Geology, 14*, 780-783, 1986.

Jennings, C., and G. Saucedo, Fault activity map of California and adjacent areas with locations and ages of recent volcanic eruptions, Calif. Div. of Mines and Geol., Sacramento, 1994.

Karig, D., S. Suparka, G. Moore, and P. Hehanussa, Structure and Cenozoic evolution of the Sunda arc in the central Sumatra region, *AAPG Mem., 29*, 223-237, 1979.

Karig, D., M. Lawrence, G. Moore, and J. Curray, Structural framework of the fore-arc basin, NW Sumatra, *J. Geol. Soc. of London, 137*, 77-91, 1980.

Katili, J., and F. Hehuwat, On the occurence of large transcurrent faults in Sumatra, Indonesia, *J. Geosci., Osaka City Univ., 10*, 5-17, 1967.

Kraeff, A., The earthquake of the Tes region, Benkulen residency on March 15th, *Berita Gunung Berapi, 1*, 40-56, 1952.

Larson, K., J. T. Freymueller, and S. Philipsen, Global plate velocities from the Global Positioning System, *J. Geophys. Res., 102*, 9961-9981, 1997.

Lassal, O., P. Huchon, and H. Harjono, Extension crustale dans le detroit de la Sonde (Indonesie): Donnees de la sismique reflexion (campagne Krakatau), *Geophysics, 309*(2), 205-212, 1989.

Lawson, A., et al., *The California Earthquake of April 18, 1906, Report of the State Earthquake Investigation Commission*, 451 pp., Carnegie Ins. of Washington, Washington, D.C., 1908.

Le Pichon, X., and J. C. Sibuet, Passive margins: A model of formation, *J. Geophys. Res., 86*, 3708-3720, 1981.

Matson, R., and G. Moore, Structural influences on Neogene subsidence in the central Sumatra fore-arc basin, in *Geology and Geophysics of Continental Margins*, edited by J. Watkins, F. Zhiqiang, and K. McMillen, pp. 157-181 , Am. Assoc. of Pet. Geol., Tulsa, Okla., 1992.

McCaffrey, R., Slip vectors and stretching of the Sumatran fore arc, *Geology, 19*, 881-884, 1991.

McCaffrey, R., Oblique plate convergence, slip vectors, and forearc deformation, *J. Geophys. Res., 97*, 8905-8915, 1992.

McCaffrey, R., P. Zwick, Y. Bock, L. Prawirodirdjo, J. Genrich, C. W. Stevens, S. S. O. Puntodewo, and C. Subarya, Strain partitioning during oblique plate convergence in northern Sumatra: Geodetic and seismologic constraints and numerical modeling, *J. Geophys. Res.*, this issue.

McCarthy, A., and C. Elders, Cenozoic deformation in Sumatra: Oblique subduction and the development of the Sumatran fault system, in *Petroleum Geology of Southeast Asia*, edited by A. J. Fraser, S. J. Matthews, and R. W. Murphy, *Geol. Soc. Spec. Publ., 126*, 355-363, 1997.

McKenzie, D., Some remarks on the development of sedimentary basins, *Earth Planet. Sci. Lett., 40*, 25-32, 1978.

Molnar, P., and P. Tapponnier, Cenozoic tectonics of Asia: Effects of a continental collision, *Science, 189*, 419-426, 1975.

Muller, J. J. A., De verplaasting van eenige traiangulatie pilaren in de residentie Tapanuli (Sumatra) tengevolge de aardbeving van 17 Mei 1892, *Natuurwet. Tijdscht. Ned. Indie., 54*, 299-307, 1895.

Natawidjaja, D., Quantitative geological assessments of Liwa earthquake 1994, paper presented at Annual Convention, Indonesian Assoc. of Geophys. (HAGI), Bandung, Indonesia, 1994.

Natawidjaja, D., Y. Kumoro, and J. Suprijanto, Gempa bumi tektonik di daerah Bukit tinggi - Muaralabuh: hubungan segmentasi sesar aktif dengan gempa bumi tahun 1926 dan 1943, paper presented at Annual Convention, Geoteknologi-LIPI, Bandung, Indonesia, 1995.

Newcomb, K. R, and W. R. McCann, Seismic history and seismotectonics of the Sunda Arc, *J. Geophys. Res., 92*, 421-439, 1987.

Nishimura, S., Re-examination of the fission-track ages of volcanic ashes and ignimbrites in Sumatra, in *Physical Geology of Indonesian Island Arcs*, edited by S. Nishimura, pp. 148-153, Kyoto Univ., Kyoto, Japan, 1980.

Nishimura, S., J. Nisida, T. Yokoyama, and F. Hehuwat, Neotectonics of the Strait of Sunda, Indonesia, *J. Southeast Asia Earth Sci., 1*, 81-91, 1986.

Pacheco, J., and L. Sykes, Seismic moment catalog of large, shallow earthquakes, 1900-1989, *Bull. Seismol. Soc. Am.., 82*, 1306-1349, 1992.

Page, B. G. N., J. D. Bennett, N. R. Cameron, D. M. Bridge, D. H. Jeffery, W. Keats, and J. Thaib, A review of the main structural and magmatic features of northern Sumatra, *J. Geol. Soc. London, 136*, 569-579, 1979.

Peter, G., L. Weeks, and R. Burns, A reconnaissance geophysical survey in the Andaman Sea and across the Andaman-Nicobar Island area, *J. Geophys. Res., 71*, 495-509, 1966.

Pramumijoyo, S., and M. Sebrier, Neogene and Quaternary fault kinematics around the Sunda Strait area, Indonesia, *J. Southeast Asian Earth Sci., 6*, 137-145, 1991.

Prawirodirdjo, L., A geodetic study of Sumatra and the Indonesian region: Kinematics and crustal deformation from GPS and triangulation, Ph.D. Thesis, Univ. of Calif., San Diego, 2000.

Prawirodirdjo, L. et al., Geodetic observations of interseismic strain segmentation at the Sumatra subduction zone: *Geophys. Res. Lett. 24*, 2601-2604, 1997.

Prawirodirdjo, L., Y. Bock, J. Genrich, S. S. O. Puntodewo, J. Rais, C. Subarya , and S. Sutisna, One century of tectonic deformation along the Sumatra fault from triangulation and Global Positioning System surveys, *J. Geophys. Res.*, this issue.

Prentice, C. Earthquake Geology of the Northern San Andreas Fault near Point Arena, California, Ph.D. thesis, California Institute of Technology, Pasadena, 1988.

Reid, H., Sudden earth movements in Sumatra in 1892, *Bull. Seismol. Soc. of Am. Bulletin, 3*, 72-79, 1913.

Research Group for Active Faults, *Main Active Faults in and Around Japan*, University of Tokyo Press, Tokyo, 1980.

Rock, N. M. S., D. T. Aldiss, J. A. Aspden, M. C. G. Clarke, A. Djunuddin, W. Kartawa, Miswar, S. J. Thompson, and R. Whandoyo, The geology of the Lubuksikaping quadrangle, Sumatra, report, 60 pp. and map, Geol. Res. and Dev. Cent., Bandung, Indonesia, 1983.

Samuel, M. A., and N. A. Harbury, The Mentawai fault zone and deformation of the Sumatran forearc in the Nias area, in *Tectonic Evolution of Southeast Asia*, edited by R. Hall and D. J. Blundell, *Geol. Soc. Spec. Publ. 106*, 337-351, 1996.

Samuel, M., N. Harbury, A. Bakri, F. Banner, and L. Hartono, A new stratigraphy for the islands of the Sumatran forearc, Indonesia, *J. Asian Earth Sci., 15*, 339-380, 1997.

Saroglu, F., O. Emre, and I. Kuscu, Active fault map of Turkey, Gen. Dir. of Miner. Res. and Explor. (MTA), Ankara, Turkey, 1992.

Sieh, K., Slip along the San Andreas fault associated with the great 1857 earthquake, *Bull. Seismol. Soc. Am., 68*, 1421-1428, 1978.

Sieh, K., Y. Bock, and J. Rais, Neotectonic and paleoseismic studies in west and north Sumatra, *Eos Trans. AGU 72*(44), Fall Meet. Suppl., 460, 1991.

Sieh, K., J. Zachariasen, Y. Bock, L. Edwards, F. Taylor, and P. Gans, Active tectonics of Sumatra, *Geol. Soc. Am. Abstr. Programs, 26*, A-382, 1994.

Smith, W. H. F., and D. T. Sandwell, Global seafloor topography from satellite altimetry and ship depth soundings, *Science, 277*, 1956-1962, 1997.

Soetarjo, U., E. Arnold, R. Soetadi, S. Ismail, and E. Kertapati, *Ser. Seismol.*, vol. 5, 199 pp., *Indonesia*, Southeast Asian Assoc. of Seismol. and Earthquake Eng., (SEASEE), Series Editor and Program Coordinator: E.P. Arnold, USGS Denver, Colo., 1985.

Stehn, C., Explosionen des Pematang Bata in der Suoh-senke (sud Sumatra) im jahre 1933, *Natuurwet. Tijdschr. Ned. Indie, 94*, 46-68, 1934.

Tapponnier, P., and P. Molnar, Active faulting and tectonics in China, *J. Geophys. Res., 82*, 2905-2930, 1977.

Tikoff, B., Sunda-style tectonics and magmatic arc processes, *Eos Trans. AGU, 79*(45), Fall Meet. Suppl., F222, 1998.

Tjia, H., Tectonic depression along the transcurrent Sumatra fault zone, *Geol. Indonesia, 4*(1), 13-27, 1977.

Tregoning, P., F. K. Brunner, Y. Bock, S. S. O. Puntodewo, R. McCaffrey, J. F. Genrich, E. Calais, J. Rais, and C. Subarya, First geodetic measurement of convergence across the Java trench, *Geophys. Res. Lett., 21*, 2135-2138, 1994.

Untung, M., N. Buyung, E. Kertapati, Undang, and C. Allen, Rupture along the Great Sumatran fault, Indonesia, during the earthquakes of 1926 and 1943, *Bull. Seismol. Soc. Am., 75*, 313-317, 1985.

Van Bemmelen, R., *The Geology of Indonesia*, 732 pp., Gov. Print. Off., The Hague, Netherlands, 1949.

Visser, S., Inland and submarine epicentra of Sumatra and Java earthquakes: Koninklijk Magnetisch en *Meteorologisch Observatorium te Batavia, 9*, 1-14, 1922.

Visser, S., De aardbevingen in de Padangse Bovalanden, *Natuurwet. Tijdschr. Ned. Indie., 87*, 36-71, 1927.

Weeks, L., R. Harbison, and G. Peter, Island arc system in the Andaman Sea, *Am. Assoc. Pet. Geol. Bull., 51*, 1803-1815,1967.

Westerveld, J., Eruptions of acid pumice tuffs and related phenomena along the Great Sumatran fault-trough system, in *Proceedings of the Pacific Science Congress*, vol. 2, Pacific Science Congress, New Zealand, 1953.

Widiwijayanti, C., J. Deverchere, R. Louat, H. Harjono, M. Diament, and D. Hidayat, Analysis of the aftershock sequence of the Mw 6.8 Liwa earthquake, Indonesia, *Geophys. Res. Lett., 23*, 3051-3054, 1996.

Yeats, R., K. Sieh, and C. Allen, *The Geology of Earthquakes*, 568 pp., Oxford Univ. Press, New York, 1997.

Zachariasen, J., and K. Sieh, The transfer of slip between two en echelon strike-slip faults: A case study from the 1992 Landers earthquake, southern California, *J. Geophys. Res., 100*, 15,281-15,301, 1995.

Zachariasen, J., K. Sieh, F. W. Taylor, R. L. Edwards, and W. S. Hantoro, Submergence and uplift associated with the giant 1833 Sumatran subduction earthquake: Evidence from coral microatolls, *J. Geophys. Res., 104*, 895-919, 1999.

Zen, M., Jr., D. Dahrin, M. Diament, H. Harjono, K. Karta, C. Deplus, M. Gerard, O. Lassal, J. Malod, and A. Martin, Mantawai-90 cruise result: The Sumatra oblique subduction and strike slip fault zones, in *Geodynamic Processes in the Forearc Sliver Plate and General Topics*, edited by H. Prasetyo, p. 46, Indonesian Assoc. of Geophys., Bandung, 1991.

D. Natawidjaja and K. Sieh, Seismological Laboratory, California Institute of Technology, Pasadena, CA 91125. (danny@gps.caltech.edu; sieh@gps.caltech.edu)

(Received April 21, 1999; revised March 3, 2000; accepted April 7, 2000.)